# Projects Conference

## Abstracts


BME Faculty of Biomedical Engineering
TECHNION - Israel Institute of Technology

June 2022

Dear all,

We are proud and honored to welcome you to take part in the: ***Annual Project Presentation Conference 2022 of the Biomedical Engineering Faculty***.

This meeting culminates a yearlong research and development experience of our 4th year students. There is a say in Hebrew tradition: "אין חכם כבעל ניסיון", meaning "Experience brings wisdom". This in a nut shell, is what the projects are all about.

During their project development experience, our students had to undergo through all the stages needed to make an idea come true. Starting with a medical problem which they had to tackle, they had to strain their imagination and think "out of the box" in order to come up with a plausible new solution. Then, they had to combine the knowledge they gained during their studies. This knowledge encompasses all the aspects of biomedical engineering, i.e. combining medical background with engineering skills and scientific knowledge. All this package had to be implemented in order to provide a real world solution.

We believe that this hands-on experience exposed and prepared our graduates to the high tech biomedical industry and to a wide variety of biomedical research in a very strong way encouraging multidisciplinary work that is vital for the students' future career, and in addition potentially foster their entrepreneurship skills.

In this booklet the abstracts of all presented projects are displayed for your perusal. We are sure that the students are eager to present the outcome of their year-long projects. We wish all of them rewarding careers after graduation. We hope that very soon they will take an active part in similar projects as professional mentors from both the industry and academia.

Kindest Regards,

Prof. Haim Azhari, Faculty Dean

Prof. Netanel Korin, Vice Dean for Undergraduate Studies and the Course Instructor

Dr. Firas Mawase, Course Instructor

# List of abstracts

## (1) Channel Selection for Seizure Prediction

Noam Zoref[1], Avery Burrows[1], Noam Keidar[1], Galya Segal[1], Rotem Shapira[1], Yael Yaniv[1]
[1] Faculty of Biomedical Engineering, Technion - IIT, Haifa, Israel

## (2) Uncovering The Role of Bone Marrow Vasculature in Facilitating Cardiotoxicity After Chemotherapy

Amal Giryes[1], Eliana Masoud[1], Ashish Tiwari[1], Yael Lupu-Haber[1], Janette Zavin[1], Katrien Vandoorne[1]
[1] Faculty of Biomedical Engineering, Technion - IIT, Haifa, Israel

## (3) A Machine Learning Approach to Evaluate the Significance of Signal Artifacts on Atrial Fibrillation Detection Through Wearable Technology

Wisam Salameh[1], Aseel Bsharat[1], Shany Biton[1], Joachim A. Behar[1], Jonathan A. Sobel[1]
[1] Faculty of Biomedical Engineering, Technion - IIT, Haifa, Israel

## (4) Substrate Stiffness Effect on Migration of T-Cells to Alginate Hydrogels

Esti Diskin[1], Shirel Kleiner[1], Baptiste Le Roy[2], Rachel Biton[2], Yifan Liao[2], Joshua Grolman[2]
[1] Faculty of Biomedical Engineering, Technion - IIT, Haifa, Israel
[2] Faculty of Material Engineering, Technion - IIT, Haifa, Israel

## (5) Hippocampal Atrophy Detection in Aging and Alzheimer's Disease

Carmit Mordechai[1], Ariel Lulinsky[1], Samah Khawaled[2], Moti Freiman[1]
[1] Faculty of Biomedical Engineering, Technion - IIT, Haifa, Israel
[2] Department of Applied Mathematics, Technion - IIT, Haifa, Israel

## (6) Construction of B16F10 Melanoma Knowledge Base Using Literature Extractive Search and Experimental Validation of the Derived Hypotheses

Erica Lang[1], Yara Kablan[1], Shaked Launer-Wachs[1], Merav Belenkovich[1], Yossi Shamay[1]
[1] Faculty of Biomedical Engineering, Technion - IIT, Haifa, Israel

## (7) 3D Force-Based Alternative Keyboard for Myopathic Disease Patients

Baraah Baryhe[1], Belal Awaad[1], Rotem Shapira[1], Gili Kamara[1], Firas Mawase [1]
[1] Faculty of Biomedical Engineering, Technion – IIT, Haifa, Israel

## (8) Data Augmentation for Improved Epileptic Seizure Prediction in EEG Signals

Gil Ella Gipsz[1], Anastasia Nepomnyashchaya[1], Galya Segal[1], Noam Keidar[1], Yael Yaniv[1]
[1] Faculty of Biomedical Engineering, Technion - IIT, Haifa, Israel

## (9) Advanced Personalized Image Analysis for Neural Modulation Targeting

Noam Shalem[1], Gal Carmely[1], Gil Zur[2,3], Alon Sinai[4], Firas Mawase[1], Lior Lev-Tov[4]
[1] Faculty of Biomedical Engineering, Technion - IIT, Haifa, Israel
[2] Faculty of Medicine, Technion - IIT, Haifa, Israel
[3] Department of Radiology Rambam Health Care Campus, Haifa, Israel
[4] Department of Neurosurgery Rambam Health Care Campus, Haifa, Israel

## (10) The Difference in Utilization of Executive Functions and Imagery Networks While Listening to Stories With and Without Visual Aids in Relation to Reading Abilities in Children

Michal Appel[1], Daria Hasin[1], Raya Meri[2], Tzipi Horowitz-Kraus[2]
[1] Faculty of Biomedical Engineering, Technion-IIT, Haifa, Israel
[2] Faculty of Education in Science and Technology, Technion - IIT, Haifa, Israel.

## (11) Tracking and Identification of Single Protein Molecules in Nano-Channels Using Advanced Image Processing

Hilly Goldner[1], Sharon Gilat[1], Shilo Ohayon[1], Amit Meller[1]
[1] Faculty of Biomedical Engineering, Technion - IIT, Haifa, Israel

## (12) Designing a Bioreactor Platform for Investigating How Different Flow Rates Affect the Maturation of Pancreas Organoids

Vardit Rosenthal[1], Or Ginsburg[1], Shlomit Edri[1], Merav Belenkovich[1], Shulamit Levenberg[1]
[1] Faculty of Biomedical Engineering, Technion - IIT, Haifa, Israel

## (13) Multifunctional Wearable Nanosensor for the Monitoring of $Ca^{+2}$ and $K^{+}$ in Sweat

Deema Wattad[1], Yara Jaber[1], Rawan Omar[2], Merav Belenkovich[1], Hossam Haick[2]
[1] Faculty of Biomedical Engineering, Technion – IIT, Haifa, Israel
[2] Faculty of Chemical Engineering, Technion – IIT, Haifa, Israel

## (14) 3D Printing a Human Heart Valve Scaffold

Bar Goldner[1], Carmit Kaye[1], Yevgeniy Kreinin[1], Merav Belenkovich[1], Netanel Korin[1]
[1] Faculty of Biomedical Engineering, Technion - IIT, Haifa, Israel

## (15) The Effect of Motivation on Motor Learning

Layan Gadban[1], Salma Khateeb[1], Firas Mawase[1], Yuval Shaine[1]
[1] Faculty of Biomedical Engineering, Technion - IIT, Haifa, Israel

## (16) Designing and Manufacturing Customized Devices for Bone Grafting Using 3D Printing and BonoFill Graft Characterization

Shani Nahum[1], Liron Adut[1], Merav Belenkovich[1], Yulia Shandalov Levi[2]
[1] Faculty of Biomedical Engineering, Technion - IIT, Haifa, Israel
[2] Bonus BioGroup LTD, Haifa, Israel

## (17) Spectral Imaging of Cancer Biopsies for Precision Medicine

Maya Almagor[1], Roni Baron[1], Yuval Garini[1]
[1] Faculty of Biomedical Engineering, Technion - IIT, Haifa, Israel

## (18) Automatic Detection of Epileptic Seizures' Periods Using ECG Signal

Noa Fisher[1], Ron Dayan[1], Noam Keidar[1], Galia Segal[1], Yael Yaniv[1]
[1] Faculty of Biomedical Engineering, Technion-IIT, Haifa, Israel

## (19) A Physiological-Based Computerized Model of Cardiac Activity in Mice and Humans for Drug Development and Personalized Medicine

Nitay Aspis[1], Ofek Boneh[1], Ido Weiser Biton[1], Yael Yaniv[1]
[1] Faculty of Biomedical Engineering, Technion – IIT, Haifa, Israel

## (20) Wearable Device for Epileptic Seizure Detection and Prediction

Mais Hadid[1], Sabry Assaf[1], Noam Keidar[1], Galya Segal[1]
[1] Faculty of Biomedical Engineering, Technion - IIT, Haifa, Israel

## (21) Finding A Synergistic Combination of Drugs for The Treatment of Head and Neck Cancer

Yuval Ganot[1], Smadar Alon[1], Asaf Eilon[1], Dana Meron Azagury[1], Yossi Shamay[1]
[1] Faculty of Biomedical Engineering, Technion - IIT, Haifa, Israel

## (22) Dyslexia Detection with fMRI Scans Using Machine Learning

Rotem Gatenyo[1], Emmanuelle Hadjadj[1], Nikolay Taran[2], Tzipi Horowitz-Kraus[2]
[1] Faculty of Biomedical Engineering, Technion - IIT, Haifa, Israel
[2] Faculty of Education in Science and Technology, Technion - IIT, Haifa, Israel

## (23) "Tumorosomes"- Tumor Biomimetic Nanoparticles for Triple-Negative Breast Cancer Targeting

Ofri Vizenblit[1], Noga Erez[1], Assaf Zinger[2,3]
[1] Faculty of Biomedical Engineering, Technion - IIT, Haifa, Israel
[2] Faculty of Chemical Engineering, Technion - IIT, Haifa, Israel
[3] Cardiovascular Sciences and Neurosurgery Departments, Houston Methodist Academic Institute, TX, USA

## (24) Machine Learning Based Analysis of Spatial Behavior as A Biomarker for Aging

Hiba Abu-Rajab[1], Asael Melchior[1], Moti Freiman[1], Michal Isaacson[2]
[1] Faculty of Biomedical Engineering, Technion - IIT, Haifa, Israel
[2] Haifa University, Israel

## (25) Non-Invasive Monitoring and Detection of Arterial Stenosis Severity and Location – A Clinical Feasibility Study

Dana Farah[1], Fadi Haddad[1], Tomer Heitner[1], Amir Landesberg[1]
[1] Faculty of Biomedical Engineering, Technion - IIT, Haifa, Israel

## (26) Investigating Microparticles for Biophysical Targeting of Abdominal Aortic Aneurysms

Perla Namour[1], Ido Rachbuch[1], Moran Levi[1], Yevgeniy Kreinin[1], Merav Belenkovich[1], Netanel Korin[1]
[1] Faculty of Biomedical Engineering, Technion - IIT, Haifa, Israel

## (27) Gait Tracking with Wearable IMU Sensors

Keren Ashour[1], Avital Spector[1], Hilik Harari[2], Merav Belenkovich[1], Zvika Shinar[3]
[1] Faculty of Biomedical Engineering, Technion - IIT, Haifa, Israel
[2] GaitBetter – wellness and fitness services
[3] MindUP – digital health incubator

## (28) Finite Element Modeling of the Mechanical Interactions Associated with Cancer Cell Invasiveness

Lana Abdelghafer[1], Razan Zoabi[1], Marina Tulchinsky[1], Daphne Weihs[1]
[1] Faculty of Biomedical Engineering, Technion - IIT, Haifa, Israel

## (29) Detection of Peripheral Arterial Stenosis by Non-Invasive Quantification of Perfusion Dynamics Utilizing Exercise Test

Hai Tkach[1], Shir Plotkin[1], Tomer Heitner[1], Amir Landsberg[1]
[1]Faculty of Biomedical Engineering, Technion - IIT, Haifa, Israel

## (30) Middle-Ear Fluids Classification via Spectrally Encoded Endoscopy for Otitis Media Screening

Shira Weinrauch[1], Bar Davids[1], Matan Hamra[1], Merav Belenkovich[1]
[1]Faculty of Biomedical Engineering, Technion - IIT, Haifa, Israel

**(1)**

# Channel Selection for Seizure Prediction

Noam Zoref[1], Avery Burrows[1], Noam Keidar[1], Galya Segal[1], Rotem Shapira[1], Yael Yaniv[1]

[1] Faculty of Biomedical Engineering, Technion - IIT, Haifa, Israel

**Introduction:** Epilepsy, a condition that causes frequent seizures, is highly prevalent, affecting approximately 1.2% of the total world population. Epileptic seizures, resulting from irregular electrophysical activity in the brain, occur suddenly and can be life-threatening if unexpected. Focused treatment of seizures before they take place could prevent their occurrence along with any resulting consequences to the patient. A wearable device for continuous recording and analysis of brain activity would be ideal for seizure prediction. Current methods of monitoring seizures usually require a complete multi-channel EEG. The full EEG hat is unrealistic for daily use, both in terms of patient comfort and the required computational power for signal analysis. Here, we present a channel selection method for reducing the number of electrodes needed for seizure prediction to a maximum of 7, making daily activities with a wearable device practical and lowering needed computational power to an acceptable range for wearable computing devices.

**Methods:** We used EEG recordings of patients from Rambam hospital in Haifa as well as from an open access recordings database from Siena hospital. We proposed modeling channel selection as a supervised classification problem. Labeling EEG signals was done using extracted features from the EEG signal in overlapping time intervals of 1.5 seconds. Features used included standard deviation (STD), entropy (ENT), and detrended fluctuation (DFA). A multivariate t-test (Hotelling's $T^2$ test) was performed, on extracted features from interictal segments and preictal segments. We assumed that in channels with a clear feature value separation between preictal segments and interictal segments we could detect preictal segments, and thus predict seizures. Up to 7 channels were selected from each recording, based on the highest $T^2$ statistics. Labeled channel data was used to train a supervised Random Forest classification model. Model data for each channel was statistical measures describing feature values calculated in a 10-minute interval of interictal segments. Model performance was evaluated using F1, sensitivity and false discovery rate, to ensure minimal selection of irrelevant channels.

**Results:** Our channel selection model, using data from both hospitals, predicted relevant channels with sensitivity of 0.6 and F1 score of 0.54. The false discovery rate was 0.51, meaning that chosen channels were 49% likely to be truly relevant.

**Conclusions:** Our channel selection method could be used in seizure prediction, making the calculations feasible for a wearable device. Using more features for each channel, as well as using advanced methods to control false discovery rate, could improve model performance. Future work may also include using a neural network for channel selection.

**Keywords:** channel selection; seizure prediction; epilepsy; EEG.

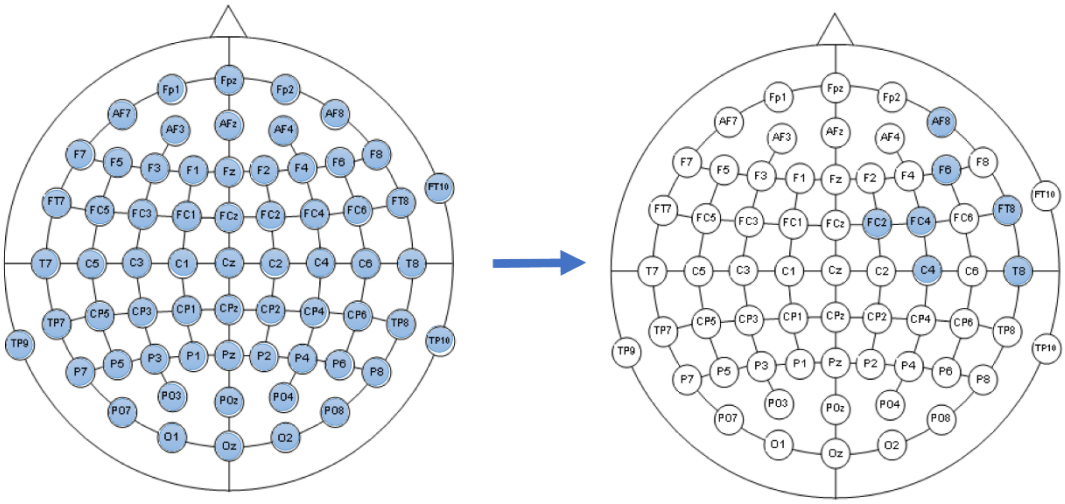


**Figure 1 – EEG channel selection.** Selected channels out of a full EEG. Using channel selection, the number of EEG channels recorded and analyzed is reduced from over 50 channels to 7.

**(2)**

# Uncovering The Role of Bone Marrow Vasculature in Facilitating Cardiotoxicity After Chemotherapy

Amal Giryes[1], Eliana Masoud[1], Ashish Tiwari[1], Yael Lupu-haber[1], Janette Zavin[1], Katrien Vandoorne[1]

[1]Faculty of Biomedical Engineering, Technion - IIT, Haifa, Israel

**Introduction:** Apart from treating cancer, anti-cancer therapy can bring about fatal cardiovascular events. 5-fluorouracil (5-FU) is the second most common chemotherapeutic drug associated with cardiotoxicity. Although it is clear that the microenvironment of bone marrow is crucial for the development of cardiovascular disease after cancer therapeutics, the role of the altered bone marrow vasculature and heart microenvironment is largely unknown. We hypothesize that this can be due to fluctuations of leukocytes in the blood released from the bone marrow niches produced from hematopoietic stem cells. Microscopic imaging techniques will be used to assess the vascular changes in bone marrow niches after 5FU administration and further subsequent effects in the heart microenvironment will be evaluated to validate our hypothesis. We anticipate that the outcome of this work would help to understand the role of the bone marrow microenvironment in chemotherapy-induced cardiotoxicity.

**Methods:** Mice (n=10) were injected with a dose of 150 mg/kg of 5-FU. On day 14 after injection, to probe permeability mice were injected with an indwelling tail vein catheter of bovine serum albumin (BSA) labeled with RhoB 16 minutes before euthanizing. To probe vessel density, 1min before euthanizing FITC-albumin was injected. Femurs and hearts were isolated, fixed and immersed in sucrose and embedded in OCT before cryosectioning. Spinning disk microscope was used to image the metaphysis of the femur with a magnification of 20x and a midventricular cardiac slice with a magnification of 10x. Analysis was done on ImageJ and for three regions of interest (ROI) used maximal intensity projection of Z stack to generate a threshold image of the bone marrow vasculature and quantify, using the tracer, the percent area occupied in the field of view 100um x 100um.

**Results:** Femur and Heart of 5FU treated mice and control mice were imaged under the microscope and we estimated the % intensity of both BSA-FITC and BSA-RhoB in the bone marrow niches and in the heart. Graphs below show the calculated % area with an average of 3 ROIs per mouse. The results show high % intensity of BSA-RhoB in the Heart and Femur of 5-FU treated mice than control mice. However, a less % intensity of BSA-FITC was estimated in the Heart and Femur of 5-FU treated mice than control mice.

**Conclusion:** It is established in the literature that after chemotherapeutic treatment, leukocytes' number and production reach a peak after 14 days, which may indicate changes that occur in the bone marrow. Our results indicate an increase in the permeability of the blood vessels and changes in the bone marrow environment.

Leaky vasculature causes more production of monocytes which may lead to cardiotoxicity (plaque formation and cardiac problems). So, Understanding and monitoring bone marrow vasculature may provide a key to unlocking therapeutic targets regulating systemic inflammation.

**Keywords:** Cardiotoxicity, 5-fluorouracil, Chemotherapy, Permeability.

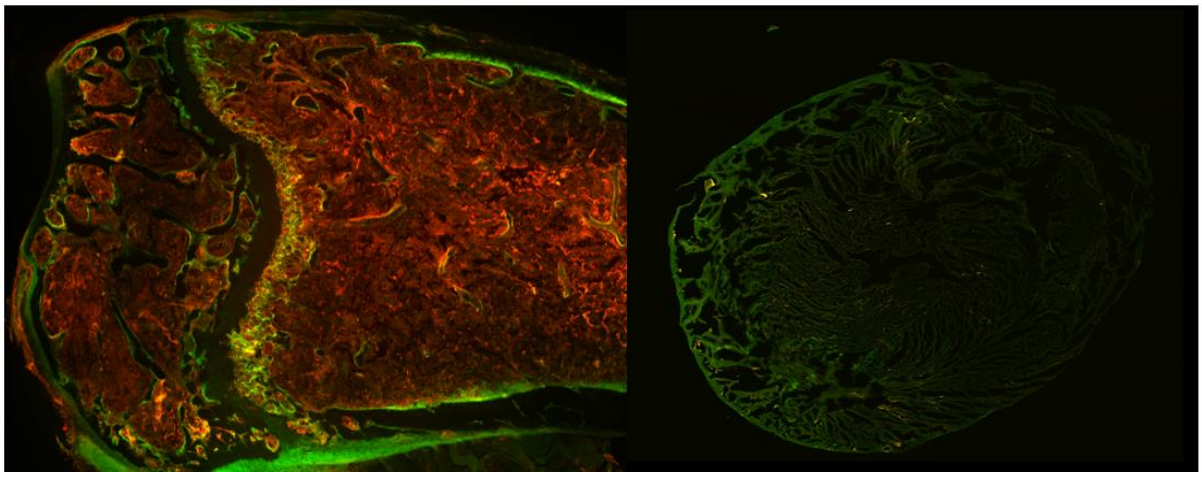

**Figure 1.** (A) Confocal images 20x objective RohB outside the blood vessels and FITC inside the vessels in the femur. (B) Confocal images 10x objective RohB outside the blood vessels and FITC inside the vessels in the heart.

**(3)**

# A Machine Learning Approach to Evaluate the Significance of Signal Artifacts on Atrial Fibrillation Detection Through Wearable Technology

Wisam Salameh[1], Aseel Bsharat[1], Shany Biton[1], Joachim A. Behar[1], Jonathan A. Sobel[1]

[1]Faculty of Biomedical Engineering, Technion - IIT, Haifa, Israel

**Introduction:** Arrhythmia is an abnormal cardiac rhythm that affects the pattern and rate of the heartbeats. Among the various arrythmia conditions, atrial fibrillation (AFib), characterized with uncoordinated atrial contraction, is the most prevalent arrythmia encountered in clinical practice. The rising popularity of wearable devices based-photoplethysmography (PPG) technology as an alternative to heart rate monitoring can potentially increase the early detection of cardiac abnormalities and facilitate their monitoring. Nevertheless, PPG-based monitoring is highly susceptible to artifacts and unwanted noise. the high susceptibility to artifacts deems PPG-based monitoring to be inherently less accurate than conventional electrocardiography (ECG) monitoring techniques. Therefore, PPG-based technology requires further investigation into the factors affecting the detection of cardiac abnormalities. In this study, we investigate the effects of the main artifacts encountered in raw PPG recordings on the machine learning algorithm's ability to detect atrial fibrillation.

**Methods:** We start the study by the generation of 735 PPG signals with ranging AFib burdens, creating a total of 125-hour long PPG recordings database. The main types of noise encountered in PPG were added to each signal in our database in varying intensities- electromyographic (EMG) noise, motion artifacts, PPG-sensor displacement, white noise, pink noise, and baseline wandering. The signals were labeled according to varying signal to noise ratio (SNR). The next step was assessing the quality of a given raw PPG signal by calculating the Signal quality index (bSQI). Signals with a signal to noise ratios (SNR) which led to a bSQI score of less than 0.8 were viewed as unfit for an accurate heart rate detection. For the classification task, a total of 15 features were utilized based on the HR time series, and three different types of machine learning classifiers were evaluated, namely logistic regression (LR), support vector machine (SVM) and random forest (RF). For performance analytics and comparison, we tested the algorithm's ability to detect AFib on different levels of SNRs, with the total range of SNR being [0.5, 20]. A secondary comparison was done with the addition of a band pass filter (BPF) and bSQI threshold as a data preprocessing step.

**Results:** The best performance metrics for AF detection was received, as expected, for the signals with no noise, while the most consistent performance was for SNR range of [15,20]. Further analysis is required, for a better understanding of the effects of artifacts for the detection of AF.

**Conclusions:** A decrease in signal-to-noise ratio affected somewhat the detection of atrial fibrillation. The highest SNR [20-15] was the most consistent with the AFib detection of a signal with no noise, and the performance of the ML models on SNR [0.5-1] was the lowest.

**Keywords:** Atrial Fibrillation, Machine Learning, photoplethysmography, Wearable Devices.

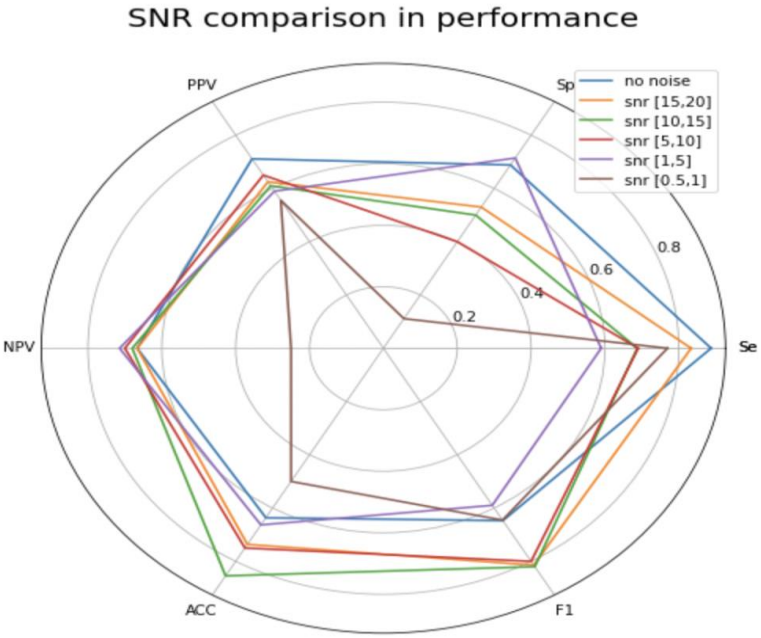


**Figure 1.** Performance metrics (Se- Sensitivity, Sp -Specificity, PPV- Positive Predictive Value, F1 Score, ACC- Accuracy, NPV- Negative Predictive Value) as radar plot.

**(4)**

# Substrate Stiffness Effect on Migration of T-Cells to Alginate Hydrogels

Esti Diskin[1], Shirel Kleiner[1], Baptiste Le Roy[2], Rachel Biton[2], Yifan Liao[2], Joshua Grolman[2]

[1] Faculty of Biomedical Engineering, Technion - IIT, Haifa, Israel
[2] Faculty of Material Engineering, Technion - IIT, Haifa, Israel

**Introduction:** Adoptive cell therapy in cancer immunotherapy is a method that often uses engineered T cells in order to combat the disease. This type of therapy has shown promise mainly in hematological malignancies, in solid tumors the efficacy of activated T cells was shown to be low in clinical trials. This fall in efficacy from in vitro to clinical trials could be potentially attributed to the properties of the substrate the T cells were grown on. Engineered T cells are injected to the body intravenously in hopes that they will migrate to the target cells, which is why the factors that affect T cell migration are important. Certain T cells properties have been shown to be affected by substrate stiffness such as proliferation and activation.

**Methods:** We made anti-CD3/anti-CD28 alginate hydrogels with 3% and 6% of $CaSO_4$ crosslinker to achieve hydrogels with different Young's modulus. We aim for hydrogels with Young's modulus in the range of 1kPa – 30kPa since this is the range of relevant biological tissues. To verify their effective Young's modulus, we are using nanoindentation technology. In a tissue culture plate, we put two hydrogels – 3% and 6% in the same well. On day 0 we added the Jurkat cells, a cancer line of T cells that were grown on tissue culture flasks, to one row of wells and on day 4 we added to two different rows Jurkat cells that have been growing on 3% or 6% hydrogels since day 0. During the 7-day experiment, pictures of the hydrogels were taken using an inverted light microscope on day 4 and day 7. The pictures were later analyzed using ImageJ Fiji for cell confluency measurements.

**Results:** Nanoindentation measurements showed that the 3% and 6% hydrogels have a Young's modulus of 3.4kPa and 7.46kPa respectively. The following results were measured on day 7: for the cells that only grew on a tissue culture flask the 6% hydrogel was the most confluent; for the cells that previously grew on 3% hydrogels, the biggest confluency was on the 3% hydrogel; for the cells that grew on 6% hydrogels, both the 3% and 6% hydrogels didn't show any significant confluency.

**Conclusions:** Cells that were grown on 3% hydrogels before they were moved onto wells with both 3% and 6% hydrogels have shown different preference in hydrogel stiffness than those who didn't grow on a specific hydrogel beforehand. Therefore, we can see a trend that the stiffness of the substrate that the cells are grown on affects their preference of substrate's stiffness when introduced to a new environment and that indicates that the cells have mechanical memory which also influences their proliferation behavior.

**Keywords:** T cells; Mechanosensing; Alginate hydrogels; Substrate stiffness.

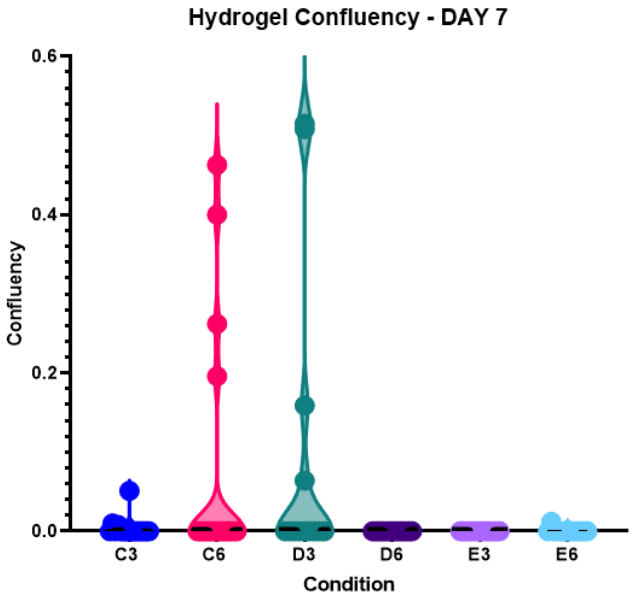


**Figure 1.** Confluency of hydrogels on day 7. C3 – 3% hydrogel, cells were added on day 0 from a tissue culture flask. C6 – 6% hydrogel, cells were added on day 0 from a tissue culture flask. D3 – 3% hydrogel, cells were added on day 4 from a 3% hydrogel. D6 – 6% hydrogel, cells were added on day 4 from a 3% hydrogel. E3 – 3% hydrogel, cells were added on day 4 from a 6% hydrogel. E6 – 6% hydrogel, cells were added on day 4 from a 6% hydrogel.

**(5)**

# Hippocampal Atrophy Detection in Aging and Alzheimer's Disease

Carmit Mordechai[1], Ariel Lulinsky[1], Samah Khawaled[2], Moti Freiman[1]

[1] Faculty of Biomedical Engineering, Technion - IIT, Haifa, Israel
[2] Department of Applied Mathematics, Technion - IIT, Haifa, Israel

**Introduction:** Alzheimer's disease (AD) is one of the most challenging health problems, leads to memory damage and cognitive impairment, which limits daily activities. Since life expectancy has grown, and aging is a major risk factor for AD, the Alzheimer's Association estimates that the number of people with AD could rise from about 26 million to more than 100 million worldwide, by 2050. AD is characterized by progressive death of nerve cells, which is reflected in a decrease in hippocampal volume. Accurate quantifying hippocampal atrophy is important to follow the course of the disease, and to assess the efficacy of new therapies.

**Methods:** Alzheimer's Disease Neuroimaging Initiative (ADNI) dataset was analyzed to find hippocampal atrophy rates. The analysis was based on T1-weighted Magnetic Resonance Imaging (MRI) of 3D brain images divided into three patient's groups: AD (n=18), mild cognitive impairment (MCI) (n=37) and healthy individuals (n=34). Each patient had 3 follow up visits, with an interval time of 1 year. First, the images were preprocessed by performing skull stripping to extract the brain wrapped by skull, resampling to uniform grid spacing and size, and intensity normalization. Further, second and third visits were aligned to first visit coordinate system by applying affine and deformable registration methods based on Advanced Normalization Tools (ANTs). Affine applies linear transformations and uses gaussian pyramid with mutual information metric, and deformable wraps the image to improve the overlap by prediction of the local deformation field, which map the pair of images into a mutual coordinate system. Finally, left and right hippocampus were extracted using pre-trained Convolutional Neural Network and Percentage Volume Change (PVC) was calculated.

**Results:** Mean baseline left and right hippocampal volumes for all the groups are summarized in Table 1. Median PVC for left and right hippocampus for the second and third visits comparing to the first visit for all the groups are summarized in Table 2.

| Volume ($mm^3$) / Group | Left | Right |
|---|---|---|
| CN | 900 | 1000 |
| MCI | 790 | 730 |
| AD | 270 | 250 |

**Table 1.** Mean left and right hippocampal volumes for the first visit (baseline) for all groups.

| PVC (%) / Group | Left | | Right | |
|---|---|---|---|---|
| | visit 2 | Visit 3 | Visit 2 | Visit 3 |
| CN | 40 | 35 | 45 | 40 |
| MCI | 35 | 50 | 30 | 15 |
| AD | 5 | -30 | 35 | -30 |

**Table 2.** Median percentage volume change for left and right hippocampus for the follow up visits for all groups.

**Conclusions:** Left and right hippocampal volumes are similar, and decreased reliance on disease severity. Generally hippocampal volume increased in the follow up visits comparing to the baseline but decreased between second and third visits. Since we found high correlation between hippocampus volumes and disease progression, we believe that early detection of AD using hippocampal atrophy rates may be possible. Yet, there is a need of larger cohort of patients to improve PVC results.

**Keywords:** Alzheimer; registration; hippocampus; volume change.

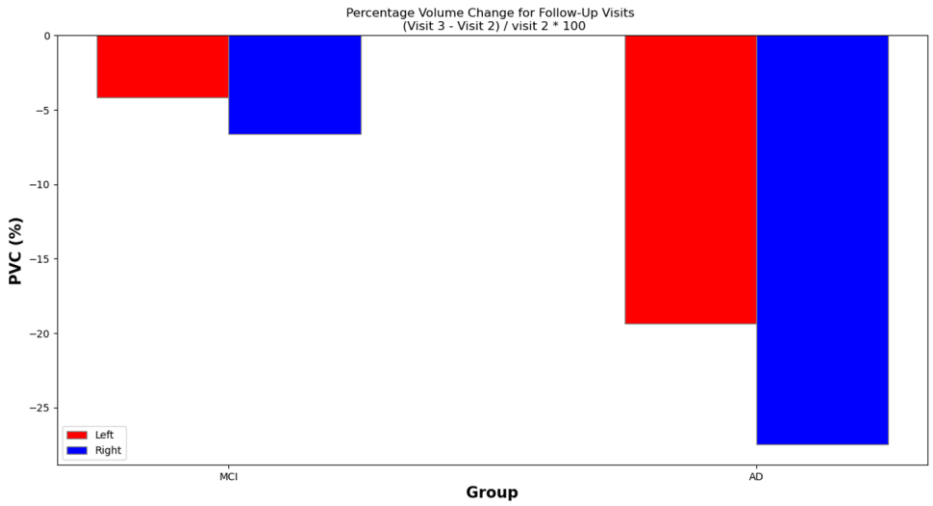


**Figure 1.** Left and right median percentage volume change of third visit comparing to the second, for MCI and AD groups.

**(6)**

# Construction of B16F10 Melanoma Knowledge Base Using Literature Extractive Search and Experimental Validation of the Derived Hypotheses

Erica Lang[1], Yara Kablan[1], Shaked Launer-Wachs[1], Merav Belenkovich[1], Yossi Shamay[1]

[1] Faculty of Biomedical Engineering, Technion - IIT, Haifa, Israel

**Introduction:** In the last decade, a huge amount of articles, experiments and theories have been published regarding different types of cancer, drugs, treatments, etc. For the purpose of coping with the information multiplicity, filtering over 10,000 articles and gathering the information needed for our study, we constructed a knowledge base specific for Melanoma and Melanoma murine cell line, B16F10. The Knowledge Base Construction (KBC) is based on Natural Language Processing (NLP) algorithms which process large datasets to understand and suggest relations between terms.

Melanoma is the most aggressive and dangerous form of skin cancer, developed from transformed melanocytes, and has high risks of growing, spreading, and leading to death. For years, the main treatment for Melanoma has been based on chemotherapy, radiation, and surgery. Lately, nanomedicine has been developed, among the rest, as a potential method for treating cancer.

**Methods:** As a head start, we constructed a database to help us map the existing studies and articles regarding B16 Melanoma. We used 'SPIKE' – an extractive search engine, using 'PubMed' articles, in order to create lists (cell-line, different names of the disease, drugs, etc…) and use them to gather information about the disease. After creating these lists, we used the 'SPIKE' search engine to build relation instances between all the lists. 'SPIKE' has generated multiple 'PubMed' articles which each pair of terms (entities) was mentioned in the same paragraph. Once a pair of entities was mentioned together in at least one article, the relation instance was captured.

In order to process and analyze the gathered relations, we imported the work to SPIKE for Knowledge Base Construction, 'SPIKE-KBC'. The instances of relations between the entities were examined, filtered and added to an interactive network tree, which represents our database. Each layer represents a different class of entities (such as Cell-Line), connected to the previous by citations (i.e. B16 – BRAF – Rapamycin).

Based on these hypotheses, we selected different drugs for experimental validation using *in vitro* drug-screening, LionHeart microscopy for cell count and MTT assay for cell viability. The most effective drugs were then combined and tested as free-drugs and as nanoparticles.

**Results:** Using 'SPIKE' and 'SPIKE-KBC', we have created a 'B16 Melanoma'-focused database, mapping relations between 6 biomedical classes: Disease (9), Cell Line (6), Gene (59), Drug (71), Ligand (28), Target (101).

Using the 'SPIKE-KBC', we have generated multiple hypotheses of optional drugs for treatment to each gene. In total, we have received *218* possible hypotheses for treatment of B16 melanoma, while affecting different related genes.

According to our drug-screening experiments, the most effective drugs were *Paclitaxel*, *Rapamycin* and *Staurosporine*. Three combinations were created, however, the most effective of them was the combination of *Rapamycin and Paclitaxel* – the lowest cell viability for the lowest drug concentration, both as free-drug combination and nanoparticle.

**Conclusions:** We have created a 'Melanoma B16' knowledge-base which contains related lists of drugs, genes, etc. After the final validation, the knowledge-base shall be open for public use. As part of the evaluation of the hypotheses generated by the 'SPIKE-KBC', we have received effective drug combinations and nanoparticles *in vitro*, which proves the 'KBC' database is relevant and can be trusted.

Based on the results, the combination of *Paclitaxel* and *Rapamycin* can be a promising treatment for Melanoma B16, as suggested in the optional hypothesis generated from our database.

**Keywords:** Melanoma; Knowledge Base Construction; Natural Language Processing.

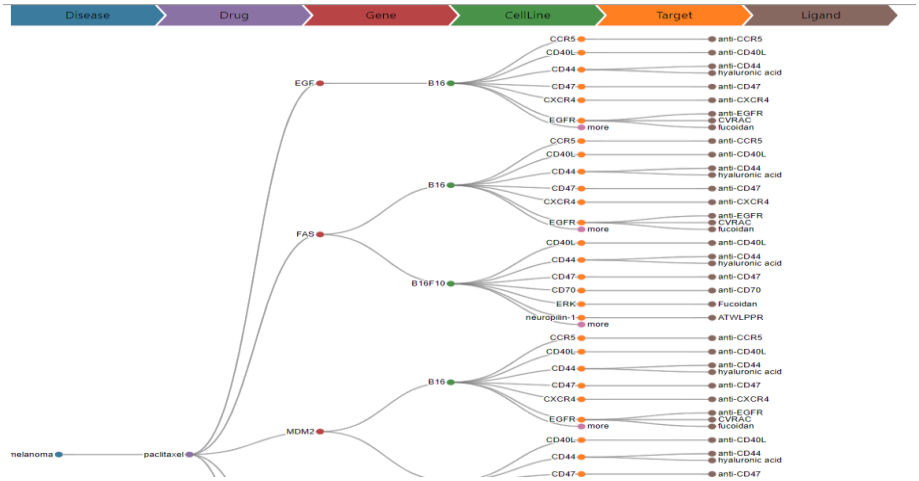


**Figure 1.** Multiple hypotheses of optional drugs.

**(7)**

# 3D Force-Based Alternative Keyboard for Myopathic Disease Patients

Baraah Baryhe[1], Belal Awaad[1], Rotem Shapera[1], Gili Kamara[1], Firas Mawase [1]

[1] Faculty of Biomedical Engineering, Technion - IIT, Haifa, Israel

**Introduction:** The main input interfaces of the computer are mouse and keyboard, which require gentle and precise finger movements. People who suffer from neurological or muscular diseases, such as muscular dystrophy, have difficulties in performing the necessary movements for standard keyboard usage. Muscular dystrophy diseases are manifested by increasing weakness accompanied by loss in muscle mass. These diseases are characterized by muscle tissue degeneration and caused by genetic mutations that interfere with protein production, which are essential for the construction and healthy function of the muscle tissue. The main difficulty of these people regarding keyboard usage is the need to perform small, delicate movements over the keyboard.

We designed and built a force sensor-based keyboard that does not require gross finger movements, but instead works by applying force in different directions. The keyboard is suitable for people with muscular degeneration diseases, by eliminating both the need to raise one's fingers in order to move them over the keyboard, and to press keys with force.

**Methods:** We designed a keyboard based on 3D FSR sensors with one sensor per finger (i.e., 5 sensors per hand). The sensors are connected to two Arduino DUE hardwares and integrated into an ergonomically designed appliance, which allows the user to place his hand and fingers comfortably and directly above the designated sensor. The designed model was then 3D printed using "Formlabs" printer with black V4 resin.

Typing is executed by rolling the fingers on top of the sensor; each roll to any distinct direction (up, down, left, and right) is encoded to force which is then processed using Arduino and a software written in C language to type a single key (i.e., 4 keys per finger). We have mapped the keyboard as follows: four sensors are designated to a set of keys according to the dexterity of each finger and the fifth sensor (thumb finger) is used for applying Space, Backspace, Newline and Caps lock.

**Results:** The 3D printed ergonomic model provided comfort and suitability for the user, eliminating the need for moving one's hand across the conventional keyboard and using force to press keys. This is accomplished by customizing the appliance to each patients' hand shape and hand placement. Moreover, taking into consideration the appliance's difference from the conventional idea of a keyboard, it was shown that accuracy and ease of usage is achieved after multiple tries and practice.

**Conclusions:** The model showed accuracy of 99.34% after six times of using the keyboard. In addition, considering that the appliance is built using affordable and approachable materials,

hardware and software enables an applicable solution that meets the basic need of typing for people who suffer from motor disabilities in their hands. This provides a proof of concept for a full keyboard.

**Keywords:** Myopathic Disease, 3D FSR Sensors, Accessibility, Keyboard.

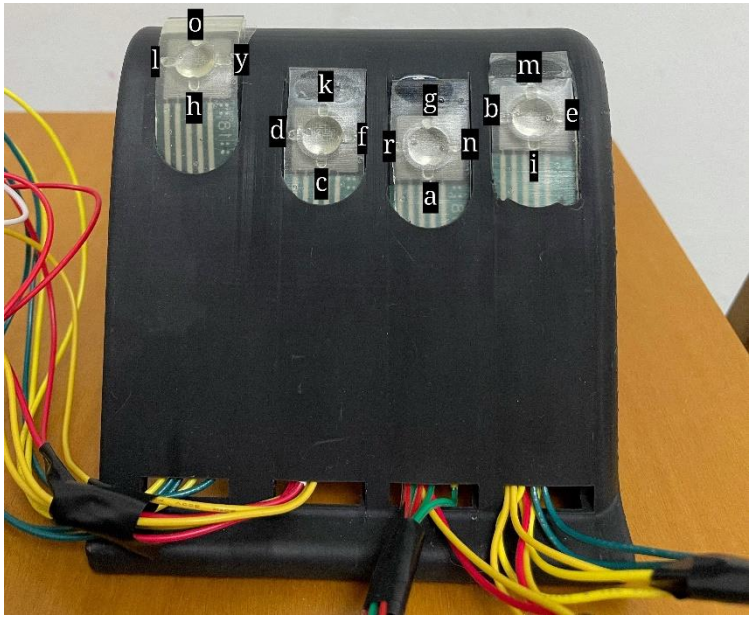


**Figure 1.** KeyFree front profile with letters mapping.

**(8)**

# Data Augmentation for Improved Epileptic Seizure Prediction in EEG Signals

Gil Ella Gipsz[1], Anastasia Nepomnyashchaya[1], Galya Segal[1], Noam Keidar[1], Yael Yaniv[1]

[1] Faculty of Biomedical Engineering, Technion - IIT, Haifa, Israel

**Introduction:** Epilepsy is a neurological disorder affecting more than fifty million individuals worldwide. The commonly used approach to diagnose it includes Electroencephalography (EEG), a recording of the patient brain's electrical activity. Currently, there is no clinically approved technology that predicts seizures, not even when the patient is in the clinic and connected to an EEG machine. The lack of such a technology has motivated efforts to design and develop automated systems that assist in the prediction of epileptic seizures.

An automated system that uses machine learning methods to predict epileptic seizures would require an abundance of EEG data, to train the algorithm. Since the existing data is very limited, due to high costs, privacy issues and the complexity of the recording process, a technique that allows artificial synthesizing of EEG recordings is necessary.

**Methods:** Data augmentation is the process of generating synthetic samples by transforming existing data, to improve the accuracy and robustness of machine learning models. Data augmentation has been demonstrated to achieve considerable performance gains — increased model accuracy, training stability and reduced train set overfitting.

Firstly, a few classical methods of data augmentation were implemented – noise addition and geometric transformation (rotation). The Gaussian noise from a multivariate normal distribution was added to the original EEG signal. The Geometric transformation method is based on the rotation of the channels with the assumption of orthogonality. At last, the vector auto regression method was implemented. The augmentation algorithm learned on signal data according to the data label – pre, mid or no seizure period. After that, the predicted fully artificially synthesized signal was assembled into one whole EEG recording. The augmentation methods were validated by a comparison of the prediction model performance with and without learning on the synthesized data.

**Results:** The results are still in the process of validation and are yet ready to be disclosed.

**Conclusions:** The data augmentation in the epileptic seizure prediction algorithm might improve the prediction performance and expand the amount of the training data. Introduction of deep learning models of augmentation may contribute further to building reliable synthetic datasets.

**Keywords:** epilepsy, data augmentation, vector autoregression, seizure prediction.

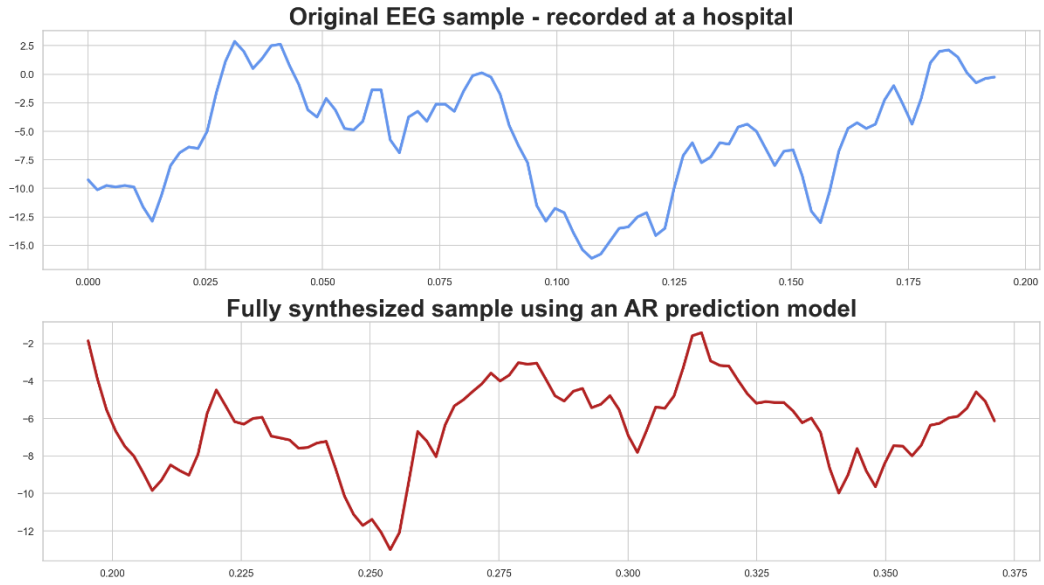


**Figure 1.** A visual comparison of a fully synthetic EEG signal, predicted with an AR model (bottom), and the original EEG signal that it was based upon (top).

**(9)**

# Advanced Personalized Image Analysis for Neural Modulation Targeting

Noam Shalem[1], Gal Carmely[1], Gil Zur[2,3], Alon Sinai[4], Firas Mawase[1], Lior Lev-Tov[4]

[1] Faculty of Biomedical Engineering, Technion - IIT, Haifa, Israel
[2] Faculty of Medicine, Technion - IIT, Haifa, Israel
[3] Department of Radiology Rambam Health Care Campus, Haifa, Israel
[4] Department of Neurosurgery Rambam Health Care Campus, Haifa, Israel

**Introduction:** Tremor is a symptom of both Essential tremor (ET) and Parkinson's disease (PD), that can lead to disability, and a dramatic reduction in quality of life, alongside social exclusion, embarrassment, and immense difficulty in performing routine tasks. Magnetic Resonance guided Focused Ultrasound Surgery (MRgFUS) is a new non-invasive technology that utilizes sound waves energy to induce a focal thermal lesion with sub-millimeter precision to treat patients with tremor. The ventral intermediate nucleus of the thalamus (VIM) is a well-studied target for tremor reduction. The common method to detect this target is based on anatomical landmarks, specifically the anterior-posterior commissure (AC-PC). This non-personalized targeting method is based on histological atlases and as a result is insensitive to anatomical differences. We will examine advanced analysis methods as stereotactic targeting approaches for personalized treatment and superior clinical outcomes.

**Methods:** Pre- and post-operative magnetic resonance imaging (MRI) scans were acquired from 56 patients who underwent MRgFUS. Using the preoperative diffusion weighted imaging (DWI) MRI sequence, three tracts (pyramidal tract [PT], medial lemniscus [ML] and dentatorubrothalamic tract [DRT]) were located for each patient using tractography, which reconstructs a 3D model of white matter pathways. The postoperative T1 weighted images of these patients were used for segmentation and volume calculation of the lesion. Geometrical measurements, such as the distance and overlap between the lesion and each of the tracts, were performed. In order to detect the factors affecting the treatment's outcome, statistical and machine learning tools were applied to find correlations between the postoperative clinical evaluation and the image analysis.

**Results:** The overlap of the lesion with a specific region of the DRT, the distance of the lesion from the ML and PT (3.3-6.3mm and 6.5mm respectively), and the total overlap between the lesion and each tract were shown to have a significant correlation to the treatment's outcome.

**Conclusions:** The treatment's target can be defined according to the correlations discovered. We suggest an innovative personalized method for detecting the MRgFUS target location. This technique tailors the target localization to a specific patient based on the spatial locations of the patient's tracts.

**Keywords:** Magnetic Resonance guided Focused Ultrasound Surgery, tractography, personalize, stereotactic targeting.

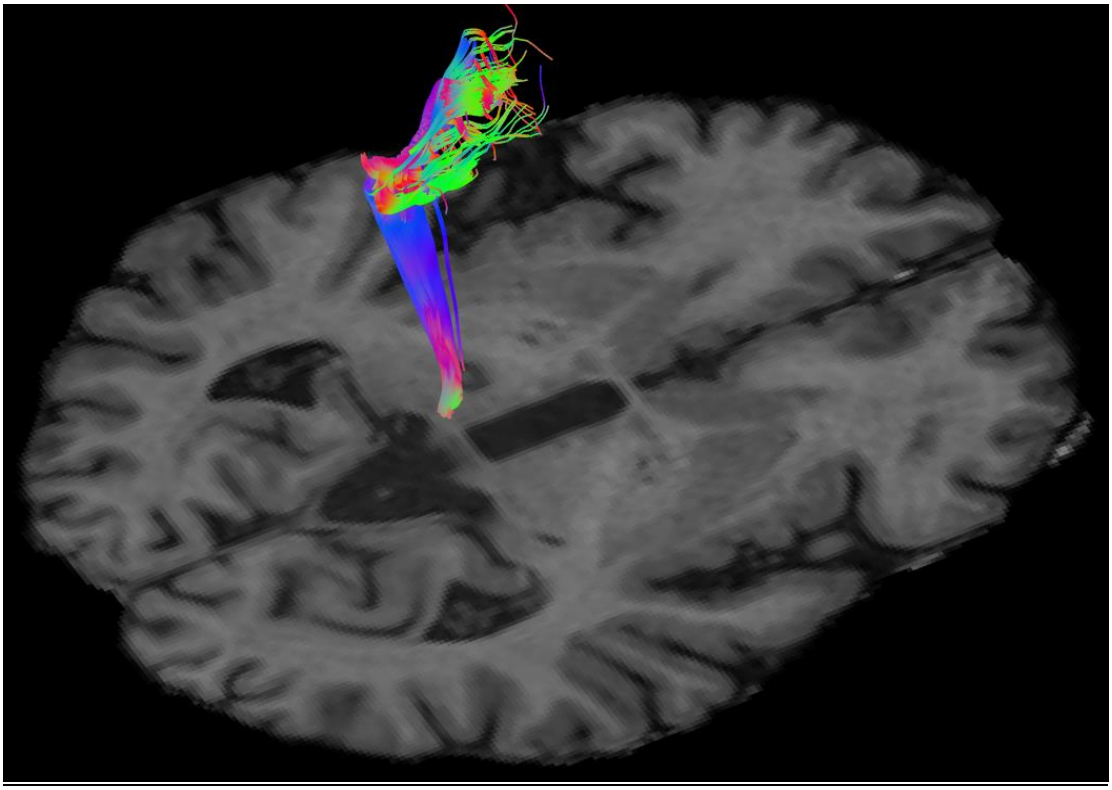

**Figure 1.** A 3-dimensional visualization of the DRT pathway traversing a postoperative T1 weighted axial slice. Streamline coloration is based on fiber orientation, where blue is superior-inferior, green is anterior-posterior, and red is left-right. Yellow arrow indicates the lesion area.

**(10)**

# The Difference in Utilization of Executive Functions and Imagery Networks While Listening to Stories With and Without Visual Aids in Relation to Reading Abilities in Children

Michal Appel[1], Daria Hasin[1], Raya Meri[2], Tzipi Horowitz-Kraus[2]

[1] Faculty of Biomedical Engineering, Technion - IIT, Haifa, Israel
[2] Faculty of Education in Science and Technology, Technion - IIT, Haifa, Israel.

**Introduction:** Reading abilities rely on basic linguistic capabilities such as narrative comprehension; both demand the utilization of Executive functions (EF) networks. Therefore, brain activation during narrative comprehension in children might be a forecast for future reading disabilities. Children with reading difficulties (or dyslexia) struggle to use their imagination and EF abilities while reading as they also rely heavily on phonological and orthographical abilities. The current study aims to determine the differences in reliance on EF and imagination processes during narrative comprehension in children and compare it to different levels of reading abilities.

**Methods:** Functional MRI scans were collected from 44 children aged 8-12 years (mean age: 9.30±1.27 years, 17 females) under two conditions: a) listening to stories without visual stimulus and; b) listening to stories while watching related pictures on a screen. Functional connectivity within and between networks associated with reading (including EF and imagination) were exported for each condition separately against word reading abilities while controlling attention. Correlation coefficient matrices were calculated for each task separately and compared using Fisher z-transformation analysis.

**Results:** Children with lower reading abilities showed greater functional connectivity between default mode network and memory network, and between auditory network and memory network for the stories without visual aids vs those visual aids. Also, comparing the full matrices, greater z scores were observed for children with higher reading abilities.

**Conclusions:** The results support the hypothesis that there is a correlation between lower reading abilities and greater difference between the two conditions (due to difficulty engaging theses basic systems compared to those with better reading ability). It also shows that greater reliance on cognitive and sensory networks is observed when visual aids are provided in those with decreased reading abilities.

We conclude that children with reading difficulties might show an improvement in their reading and narrative comprehension skills using visual aids.

**Keywords:** Functional connectivity, Narrative comprehension, Reading abilities, Executive functions.

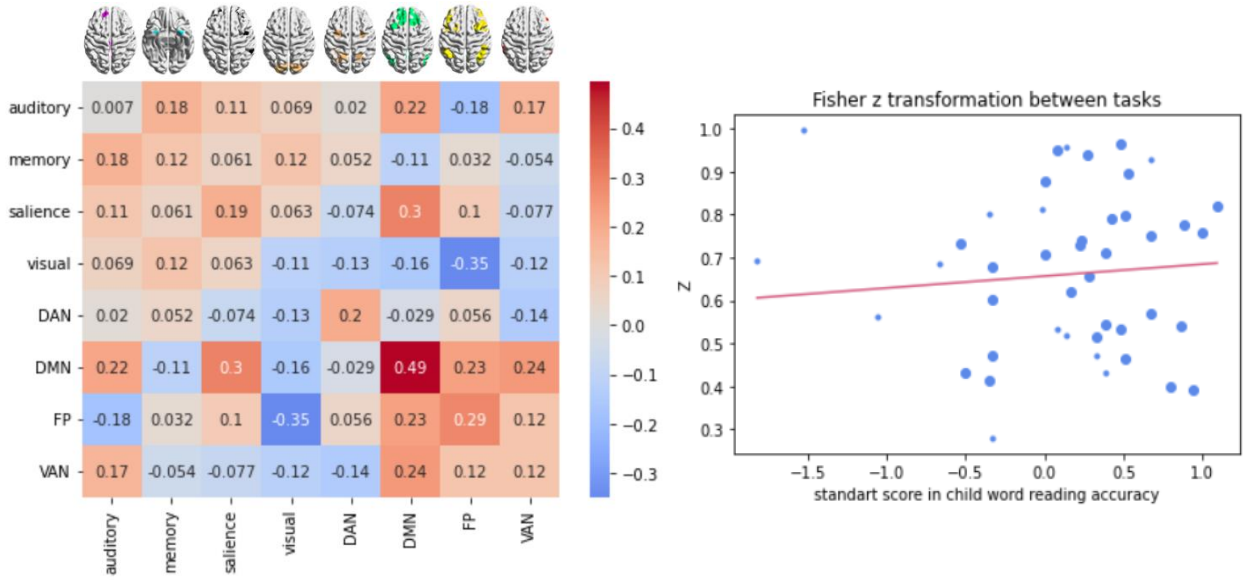


**Figure 1.** Left - the normalized correlation (z value) in functional connectivity between two tasks. Right - the normalized correlation (z value) in functional connectivity between two tasks in relation to reading abilities while controlling attention, the bigger dots represent subjects with better attention skills.

**(11)**

# Tracking and Identification of Single Protein Molecules in Nano-Channels Using Advanced Image Processing

Hilly Goldner[1], Sharon Gilat[1], Shilo Ohayon[1], Amit Meller[1]

[1] Faculty of Biomedical Engineering, Technion - IIT, Haifa, Israel

**Introduction:** Proteins are the fundamental molecular elements responsible for the function of cells and tissues. Their relative quantities may serve as clinical indicators for disease states, hence they are considered "biomarkers". Consequently, identification of proteins is a necessary tool that can improve early diagnostics and personal treatment. However, current protein mapping methods are challenged with accuracy limitations. These issues are exacerbated by the absence of protein amplification methods, which could lead to inaccurate diagnoses. There is a high need to develop an accessible, affordable, molecular-scale platform that will map all proteins accurately with single-molecule precision.

**Methods:** The count of few amino acids defines fingerprints of >70% of the human proteome. Here the idea was to create a single-molecule identification solution by extracting movement profiles of proteins and their light intensities over time in two color channels (that reflect the number of two distinct amino acids). The emitted light stems from fluorophores conjugated to specific amino acids, and it is proportional to the number of these amino acids in each protein.

Based on electrophoresis that separates proteins by mass, we used electrophoretic mobilization of dye-labeled proteins in custom-made nanometer-scale channels. Adjustments to molecular scale were achieved by running the proteins inside the device where they are restricted to 2D movement, while a sensitive optical system constantly followed their movement. The proteins appear as small moving fluorescent particles.

We created an algorithm that receives an image sequence that comprises a specific running experiment, marks proteins by finding intensity peaks and creates tracks of proteins by connecting consecutive images. The marking process is based on defining channel boundaries and threshold of relevant intensities. Creating the tracks also included physical assessments, as the fluorophores blink and cause discontinuities of intensity in time. The first track image determines the number of routes, and by evaluating the minimal Euclidean distance, each protein point was connected to another protein point in the following image.

**Results:** The results relate to Proof-of-Concept of our technology. The exploration of human proteins database and characterization of mass and amino acids count distributions enabled to create heatmaps of proteins ranges. Even in dense ranges of proteins, the data combination led to high theoretical clinical identification.

First experimental result was the algorithm-based tracks that separated between proteins and was created based on physical assessments on raw data. From the tracks of a certain single protein, advanced statistic results were achieved. Velocity and intensity histograms were

derived and fitted to Gaussians. The distribution parameters indicate the probable ranges of mass and amino-acid count related to this protein.

**Conclusions:** Nanometric channels presented high potential as a proteins identification platform, as they were useful for extraction of characteristic molecular-scale parameters. The theoretical analysis emphasized that combining levels of physical data can lead to proteins identification. Combining the spatial and intensity experimental data in time rate of seconds, enabled to define the protein velocity and intensity distributions, and therefore theoretically distinguishes between proteins in high resolution using significantly smaller samples.

**Keywords:** Proteins Identification, Single-Molecule Tracking, Nano-channels, Image-Processing.

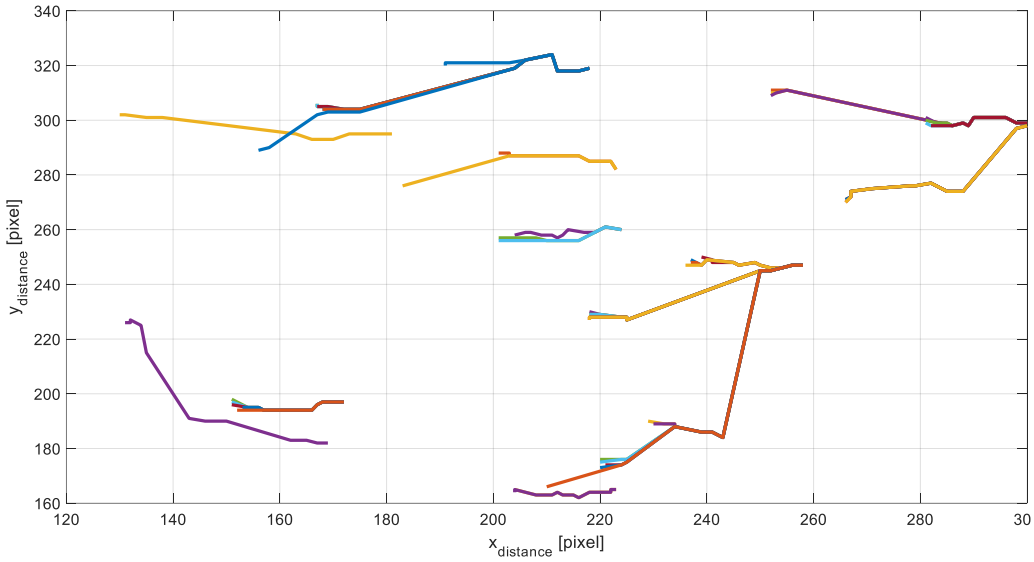


**Figure 1.** Algorithm-based tracks of one type of protein inside nano-channels device.

**(12)**

# Designing a Bioreactor Platform for Investigating How Different Flow Rates Affect the Maturation of Pancreas Organoids

Vardit Rosenthal[1], Or Ginsburg[1], Shlomit Edri[1], Merav Belenkovich[1], Shulamit Levenberg[1]

[1] Faculty of Biomedical Engineering, Technion - IIT, Haifa, Israel

**Introduction:** Organoids are stem cell derived 3D structures created through the process of cell self-organization. The organoids exhibit similar key anatomical and physiological features as their physiological counterpart organ but on a smaller scale. Therefore, organoid culture technology can potentially be a useful tool for modeling normal and pathological human organ development, as well as for demonstrating biological processes such as tissue renewal and drug screening. Particularly, pancreas organoids can be used to achieve better understanding of the development and treatment for many diseases such as cystic fibrosis, pancreatic adenocarcinoma and diabetes mellitus. The latter is among the top 10 worldwide leading causes of death according to the World Health Organization (WHO).

Currently, one of the major difficulties is achieving an advanced organoid maturity in the sense of capturing the full functional repertoire of its physiological counterpart organ. A partial solution for this is growing the differentiating stem cells with the addition of mesoderm progenitors that contribute to the vasculature of the organoid. In addition, applying flow, air interface and mechanical stimuli can improve the organoids maturation, tissue morphogenesis and homeostasis which are highly influenced by mechano-physiological parameters (such as shear stress, flow and pressure). Thus, in this research we designed a system that allows controllable flow rate that can be used for analyzing how fluid shear stress influences the maturity and vasculature development of pancreas organoids.

**Methods:** A BVOH bioreactor mold was designed using CAD software (SOLIDWORKS™ 2021) and printed in a 3D printer (PRUSA i3 MK3). Then, a PDMS bioreactor was created from the mold. The bioreactor was connected to a peristaltic pump with a volumetric flow rate of 500 µl/min. Pancreas Organoids were obtained from mouse embryonic stem cells using previously established protocols for differentiation into pancreatic progenitor cells (PPs) and organoids. After six days, the formed organoids were taken for encapsulation in Gelatin-microbial transglutaminase (mTG) gel (30 µl drops of 6.7% gelatin and of 5% mTG). The Gelatin-mTG encapsulated organoids were put in the bioreactor and in an optic 24-well plate as control group. After 3 days the organoids were fixed and prepared for immunohistochemical fluorescence staining.

**Results:** A bioreactor compatible for organoid growing under different flow rates was designed and tested successfully. We first tested the system with red dye to make sure the connection to the peristaltic pump is satisfactory. Then, we tested the system with gelatin-mTG encapsulated organoids and discovered that the resulted structure was too thick for immunostaining antibodies penetration. Thus, we could not assess the impact of the medium flow rate on the organoids maturation. In the next experiment, we will make sure the gel drops will be thinner.

For the control group, we were able to perform immunostaining and got PPs biomarkers expression for Cytokeratin 19 (CK19), E-cadherin and Sox9, among endothelial cells biomarkers expression for CD31, creating capillary network. (Figure 1(b), 1(c))

**Conclusions:** Minor changes to the bioreactor design should be applied to create a system suitable for immunohistochemical fluorescence staining. In addition, further research is needed for evaluating the impact of different medium flow rates on the organoid's maturation, vascularization and differentiation.

**Keywords:** pancreas organoids, organoid maturation, bioreactor, flow rate.

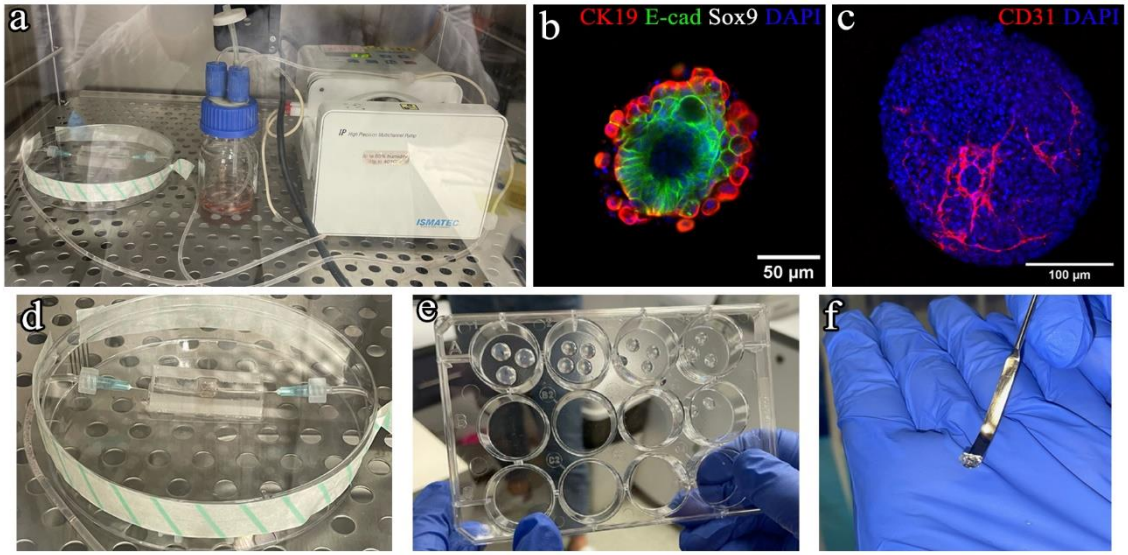


**Figure 1.** (a) Bioreactor system with gelatin-mTG encapsulated organoids connected to peristaltic pump; (b) CK19, E-cad, Sox9 and DAPI immunostaining of control group; (c) CD31 and DAPI immunostaining of control group; (d) Close-up of the bioreactor; (e) Gelatin-mTG test drops; (f) Close-up to the gelatin-mTG gel from the bioreactor.

**(13)**

# Multifunctional Wearable Nanosensor for the Monitoring of $Ca^{+2}$ and $K^+$ in Sweat

Deema Wattad[1], Yara Jaber[1], Rawan Omar[2], Merav Belenkovich[1], Hossam Haick[2]

[1] Faculty of Biomedical Engineering, Technion – IIT, Haifa, Israel
[2] Faculty of Chemical Engineering, Technion – IIT, Haifa, Israel

**Introduction:** Detection of potassium ($K^+$) and calcium ($Ca^{+2}$) levels in body fluids, especially sweat, can indicate underlying severe health problems related to the imbalance of their concentrations such as kidney failure and heart disease. The physiological concentration range in sweat for $K^+$ is 3-10mM, and for $Ca^{+2}$ the physiological concentration is $\approx 0.1mM$. So far, the detection of $K^+$ and $Ca^{+2}$ levels in the body has been conducted by laboratory tests involving complex equipment and time-consuming processes. The alternative developed in this project is a light, wearable, and minimally invasive nano sensor with high sensitivity and selectivity to both ions.

**Methods:** The first step was the synthesis of the silver nanowires (AgNWs), which are the basis of the electrodes. These electrodes are composed of 4 sensing areas: half of which are specific to calcium and the other half to potassium, and one area for electrical reference of the circuit. Hence, their conductivity was measured by digit multimeter to verify that their resistance is in magnitude order of ohm. To check the homogeneity of the microstructure of the nanowires, a microscope characterization was done.

Two solutions of the ions, one for each, in Dulbecco's phosphate-buffered saline (DPBS) were drop-casted on the sensing areas, serving as ion-selective membrane for $K^+$ and $Ca^{+2}$. Next, a Keithley 2450 System Source Meter open-circuit voltage measurement was conducted to understand the electrical behavior of the fabricated sensor.

The selectivity was evaluated by the response of $Ca^{+2}$ areas (referred to as Ca1 and Ca2 in figure 1) to 5 different concentrations of $K^+$ solutions: 1.25mM, 2.5mM, 5mM, 10mM, 20mM. Whereas the sensitivity was measured by the response of Ca1 and Ca2 to increasing concentrations of $Ca^{+2}$: 0.007mM, 0.014mM, 0.028mM, 0.056mM, 0.112mM, 0.224mM. Similarly, the selectivity of $K^+$ sensing areas (K1 and K2) was measured by their response to the previously mentioned concentrations of $Ca^{+2}$, and their sensitivity was evaluated by their response to the previously mentioned concentrations of $K^+$.

**Results:** The $Ca^{+2}$ sensing areas showed a high selectivity for calcium, which appeared through little voltage change because of increasing $K^+$ concentrations
$\Delta V = 0.020 \pm 0.001\ [V]$. Whereas they exhibited high sensitivity to increasing concentrations of $Ca^{+2}$, this was apparent in voltage change $\Delta V = 0.09 \pm 0.05\ [V]$,
namely: one magnitude order higher.

**Conclusion:** The results suggest that it is possible to monitor multiple electrolytes simultaneously through a minimally invasive wearable nanosensor with high selectivity and sensitivity, thereby allowing for real-time data collection from the patient. Hence, it aids in the early diagnosis and management of severe health problems like kidney failure and heart disease.

**Keywords:** Wearable Nanosensors, Multifunctional, Ion Monitoring, Diagnosis.


**Figure 1.** Scheme of the nano sensor with four sensing areas: K1, K2, Ca1, Ca2.

Middle area represents the electrical reference.

**(14)**

# 3D Printing a Human Heart Valve Scaffold

Bar Goldner[1], Carmit Kaye[1], Yevgeniy Kreinin[1], Merav Belenkovich[1], Netanel Korin[1]

[1]Faculty of Biomedical Engineering, Technion - IIT, Haifa, Israel

**Introduction:** Valvular heart disease, which affects approximately 2.5% of the American population, occurs when one or more heart valves (HV) fail to open and close properly, affecting the heart's efficiency. Currently, HV disease is treated with HV replacement surgery. The most commonly used replacements are mechanical and bioprosthetic HVs. Both options, however, have considerable limitations as mechanical valves require lifelong anticoagulation therapy and bioprosthetic valves present limited durability. As the demand for replacement HVs grows, it is critical to develop more customizable HVs, and Tissue Engineering (TE) may offer a novel solution. Biodegradable scaffolds provide an ideal environment for TE, where cells can multiply and cover the scaffold, so that when the scaffold eventually degenerates, the cells alone remain. Here we focus on the use of Stereolithography (SLA) 3D printing technology for TE of HV. This solution has the potential to advance the field of TE by fabricating customizable scaffolds for the regeneration of HVs with customized geometries.

**Methods:** CAD software was used to design a HV model and exported to an STL file format. A desktop SLA 3D printer was modulated to make printing possible using a bioink. The photoinitiator, Lithium phenyl (2,4,6-trimethylbenzoyl) phosphinate (LAP), which initiates a radical reaction using UV light ($405\ [nm]$), was combined with Phosphate Buffered Saline (PBS) and Polyethylene glycol diacrylate (PEGDA). PEGDA was chosen for the scaffold material because it encourages cell viability and can enable direct integration of the cells into the bioink in the future. The Young Modulus was measured using an Instron® Tensile test system. The model was prepared for printing using CHITUBOX Slicer application and the printing settings and parameters to obtain successful 3D printing were studied.

**Results:** For a composition of 20% PEGDA, 0.05% LAP, and 80% PBS, the polymer's Young Modulus was $1.65\ [MPa]$ and for a composition of 33.3% PEGDA, 0.8% LAP, and 66.6% PBS, the polymer's Young Modulus was $2.25\ [MPa]$. The optimal printing resolution was determined from a scaled-down valve model that was printed under three different UV exposure times: $20\ [sec]$, $50\ [sec]$, and $100\ [sec]$ (Figure 1).

**Conclusions:** The polymer composition which provided the most ideal results was 20% PEGDA, 0.05% LAP, and 80% PBS, due to its lower Young Modulus and greater flexibility. To achieve the highest printing resolution, the UV exposure time was set to $25\ [sec]$. Future research would produce a 3D printed HV that is durable in a flow system. Afterwards this research could combine the use of MRI and CT scan technology to offer a solution with high precision and generate patient specific therapies.

**Keywords:** valvular heart disease; SLA 3D bioprinting; biocompatible scaffold.


**Figure 1.** valvular heart disease; SLA 3D bioprinting; biocompatible scaffold.

**(15)**

# The Effect of Motivation on Motor Learning

Layan Gadban[1], Salma Khateeb[1], Firas Mawase[1], Yuval Shaine[1]

[1] Faculty of Biomedical Engineering, Technion - IIT, Haifa, Israel

**Introduction:** Motor learning which's defined as the change in the capability of a person to perform motor skills plays a significant role in our lives. Humans possess a remarkable ability to learn new motor skills throughout their life stages. It's known that motivation has a great effect on motor learning and adaptation but the scientific basis regarding is still unclear.

**Methods:** Our study is composed of a multi-phase force-field motor adaptation task. Fifteen young right-handed people without any neurological, motor, or cognitive dysfunctions performed the experiment, they weren't informed about the objectives of the study.

Participants were holding onto the handle of a robotic manipulandum and instructed to make reaching movements to move a displayed cursor from a starting position toward a target, movement were considered successful if the hand reached a velocity in the correct range that the participants learned during the experiment by giving them comments such as "move faster/slower"

Within the multi-stage approach to the study, participants first performed a baseline phase for familiarization in which no external force-field perturbations were applied. This was done in order to remove any bias coming from the physiology of our arms. Participants were then exposed to pseudo-random velocity-dependent force-field perturbations. Across trials, the perturbation magnitude was uniformly distributed and sampled. Within these perturbation trials, some trials were associated with monetary cues that were uniformly sampled, but statistically independent of the perturbation schedule [10 NIS: low motivational state, 100 NIS: high motivational state].

The code was written in visual studio using C++ language, the results were analyzed in Matlab.

**Results:** There're 3variables that need to be calculated to quantify the effect of motivation on motor adaptation: α-The retention rate, $e(n)$error that was experienced in trial $n$, $\lambda(e(n))$ adaptive response from error.

For now, we've estimated the retention rate α: by introducing additional pairs of channel trials $C1C2$ no perturbation, no motivational cues, $\alpha$ is the ratio of the forces in these two trials:

$$\alpha = \frac{f\,(n+1)}{f(n)}$$

Now we're working to estimate $e\ (n)$ and $\lambda(e(n))$, and then will approximately reflect the adaptive response to the motivational cue $M(n)$:

$\lambda\,(M(n) \mid e(n)) = \lambda(e(n), M(n)) - \lambda(e(n)) \approx k \cdot M(n) - \lambda(e(n))$, $k$ is the rate parameter. Thus, if a participant generates a motor command of a force on a given trial, we assume that this

could be related to the adaptive response to error $\lambda(e(n))$, and the adaptive response to motivation in addition to the experienced error $\lambda\,(M(n) \mid e(n))$.

**Conclusions:** We're in the right direction to quantify the effect of motivation on motor learning, there're some parameters left that need to be evaluated based on the experiments we did using Matlab, and that way we can process the results and answer this research question.

**Keywords:** Motor learning, Motivation, Adaption.

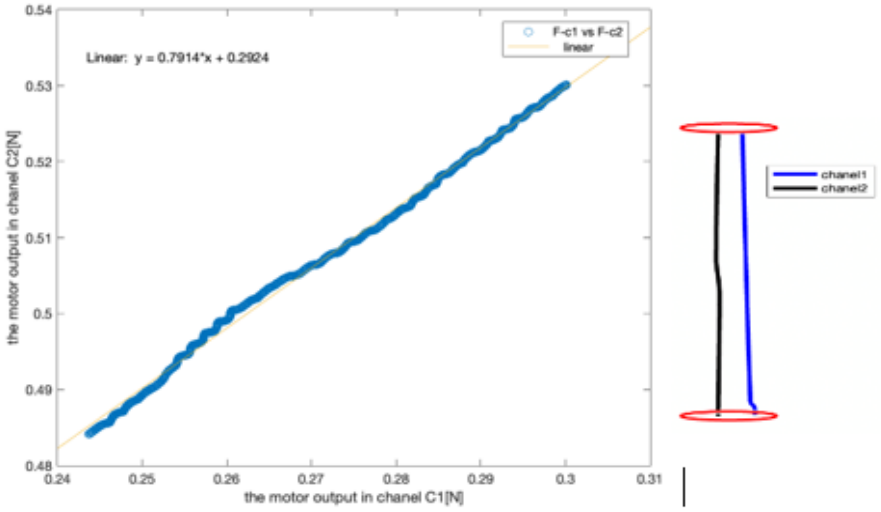


**Figure 1.** Channel pairs and the estimated retention-rate α.

**(16)**

# Designing and Manufacturing Customized Devices for Bone Grafting Using 3D Printing and BonoFill Graft Characterization

Shani Nahum[1], Liron Adut[1], Merav Belenkovich[1], Yulia Shandalov Levi[2]

[1] Faculty of Biomedical Engineering, Technion - IIT, Haifa, Israel
[2] Bonus BioGroup LTD, Haifa, Israel

**Introduction:** Bone defects might be caused by unhealed fractures or bone diseases and require reconstruction. BonoFill™ is an innovative bone graft developed by Bonus BioGroup for the treatment of bone deficiencies in the limbs and jaw. BonoFill™ consists of MSCs induced to differentiate into osteogenic cells, grown on 3D natural mineral scaffolds, and upon transplantation the cells continue to proliferate and differentiate into mature osteoblast. BonoFill™ is not firm and is transplanted by injection. The graft will reach its final shape only when cells become mature osteoblasts, which may take weeks or months after the transplantation. This may cause problems such as displacement of the graft and difficulties in making it fixated to a damaged tissue. A customized device is needed in order to overcome these problems.

**Methods:** Double cylinder-shaped cages with tiny holes were designed using SolidWorks (outer diameter: 25mm, inner diameter:7.5mm, length: 4cm, holes diameter: 1mm), and printed using a 3D printer (Original Prusa i3 MK3S+). The cages were made of Poly lactic acid (PLA), a biodegradable, FDA approved material. The cages are intended for tibial fractures and therefore were designed as a cylinder. The graft will be placed between the two cylinders to increase the surface area of the graft and by that improving nutrients supply. In vitro tests were performed next. BonoFill™ was seeded in the printed cages, and after a week of incubation we performed cell counting, cell viability assay and cell identification. The results were compared to the control group, without cage. In order to characterize BonoFill™ graft the scaffolds were inserted into a 6 -WP and then centrifuged in order to isolate the fluid that surrounds the cells. We used a rheometer to measure the viscosity of the fluid.

**Results:** The cage caused minor decreases in cell viability and Alkaline phosphatase (ALP) activity. ALP indicates differentiation into osteogenic cells. Viscosity test showed shear thinning behavior of the graft's fluid, which indicates it is a non-Newtonian fluid.

**Conclusions:** Cells are able to proliferate and differentiate when seeded in the printed cage, yet it results in reduced cell viability, reduced ALP activity and lower cell count in comparison to the control group. Design improvement is required in order to minimize the impact of the cage on nutrients supply. A design with a few single bigger holes in the outer wall of the cage will be done in future work. Satisfying results will allow preclinical research to begin.

**Keywords:** Bone Grafting, Tissue Engineering, 3D Printing.

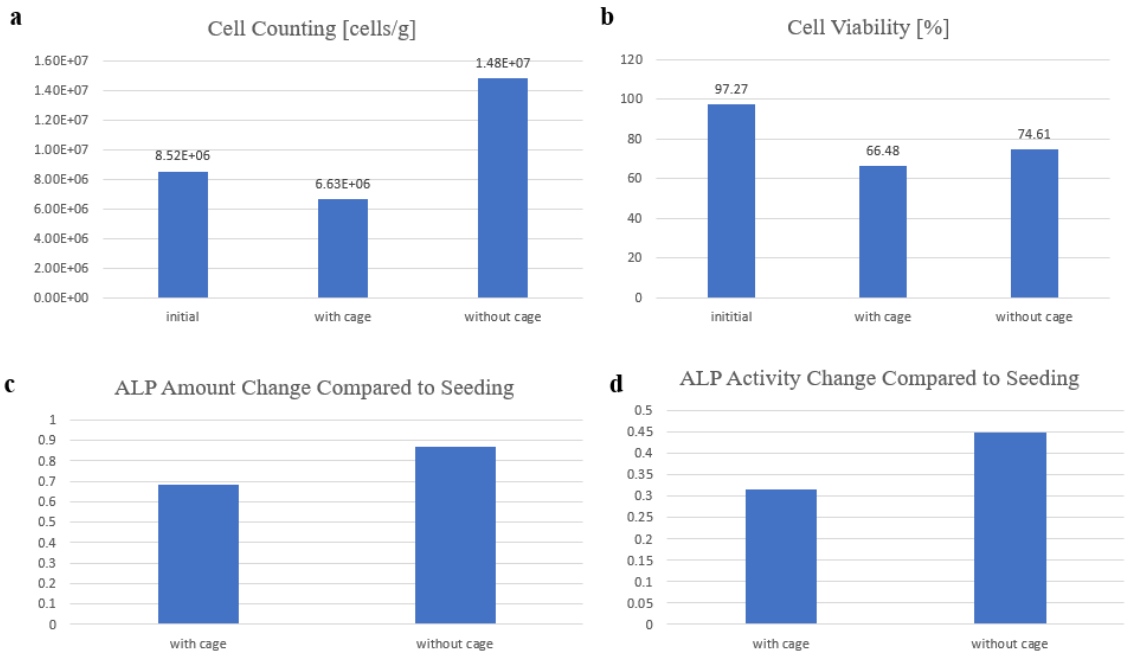


**Figure 1.** In vitro impact of the cage on BonoFill™. (a) Total cell count. (b) Viability percentage. (c) Amount of ALP in cells compared to seeding. (d) Enzymatic activity of ALP compared to seeding.

**(17)**

# Spectral Imaging of Cancer Biopsies for Precision Medicine

Maya Almagor[1], Roni Baron[1], Yuval Garini[1]

[1] Faculty of Biomedical Engineering, Technion - IIT, Haifa, Israel

**Introduction:** Precision medicine has revolutionized modern approaches to cancer treatment. Personalized drugs are effective but only for a fraction of patients, therefore biopsies must be screened in advance to assess the likelihood of success in response to the medicine. Screening of cancer biopsies requires usage of multiple labels that indicate the presence of specific proteins (biomarkers). The more proteins that can be detected, the more accurate the characterization of biopsies, so that the most suitable drug can be matched to the patient.

Generating an image of a specimen with multiple biomarkers presents a challenge. This is commonly done using fluorescence microscopy after labeling proteins with different fluorescent colors (fluorochromes). However, this is complex, as colors may overlap leading to inaccurate analysis. Most imaging systems measure each fluorochrome with a specific filter, serving most practical purposes but limited when multiple colors of similar wavelengths need to be differentiated, as measurements become time-consuming and noisy.

Here we present a novel method for identifying multiple biomarkers by using a spectral imaging optical system to extract clinical information from fluorescently labeled biopsies.

**Methods:** Our method involves three steps; staining, spectral imaging, and analysis.

For staining, we developed a multiplex immunohistochemistry protocol to evaluate pathological biopsies. Antibodies targeting Estrogen receptors, Progesterone receptors and Ki67 were used for labeling, together with DAPI to mark cell nuclei. Our process ensures a high signal for each protein.

Next, pathological slides were placed under a microscope and images were obtained by using the Fourier-based Spectral Imaging system, developed in Prof. Garini's lab. The system allows rapid scanning of samples and recording of the light spectrum within the visible range for each pixel. To optimize measurements, we designed a precise multi-band filter fitting the excitation and emission spectra of the fluorophores, allowing the single-shot capture of all spectral information.

The spectral data was then analyzed using a number of algorithms. Segmentation of nuclei and individual fluorophore-bound biomarkers in nucleic regions was performed, followed by linear decomposition of the fluorescent spectra. This allows us to quantify the concentration of each protein within the biopsy cells.

**Results:** We established a protocol for staining and detecting multiple protein-based biomarkers, using a variety of fluorescently labeled antibodies. The stained biopsies were then spectrally imaged. Multi-channel spectral separation allowed for wavelength-specific segmentation and classification of tissue components, generating a spectral signature of the

sample. This provided the basis for the extraction of protein expression profiles and the proliferation index.

**Conclusions:** We developed a unique method for efficiently generating a molecular profile of pathological biopsies, according to their spectral signature. Future research should focus on using spectral information to differentiate between healthy and cancerous cells, increasing the number of biomarkers and applying this information to improve personalized cancer medicine. We believe that this method has high generalization potential to be adapted for other applications that rely on extracting quantitative information from labeled biological samples.

Finally, to maximize treatment effectiveness, assigning personalized oncological drugs to cancer patients requires identification of multiple biomarkers, a clinical gap that our method bridges.

**Keywords:** Spectral Imaging; Cancer; Protein Profiling; Immunohistochemistry.

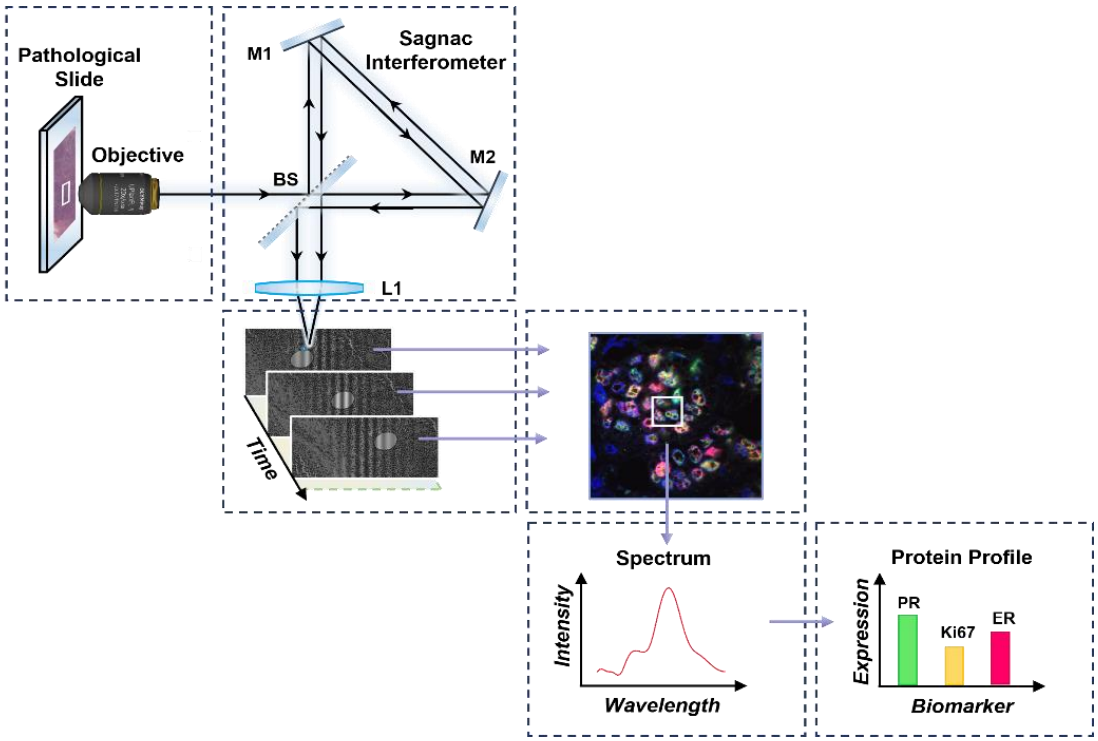


**Figure 1: Schematic diagram of the Spectral Imaging system and the analysis results.** The scanning process of a region of interest is demonstrated, followed by spectrum extraction and protein profiling.

**(18)**

# Automatic Detection of Epileptic Seizures' Periods Using ECG Signal

Noa Fisher[1], Ron Dayan[1], Noam Keidar[1], Galia Segal[1], Yael Yaniv[1]

[1]Faculty of Biomedical Engineering, Technion - IIT, Haifa, Israel

**Introduction:** An epileptic seizure is a transient occurrence of signs and/or symptoms due to abnormal excessive or synchronous neuronal activity in the brain. A person characterized by enduring predisposition to generate epileptic seizures may be diagnosed with epilepsy and suffer from neurobiological, cognitive, psychological, and social consequences of this disease. Commonly, epilepsy is diagnosed by means of electroencephalogram (EEG), which can detect changes in neuronal activity occurring during an epileptic seizure.

EEG procedure is tedious, time-consuming (especially for long recordings) and expensive since expert investigation is needed. Furthermore, as there are many different patterns of clinical and electrophysiological seizure manifestation, the elaborative investigation of ictal or interictal patterns becomes demanding and complex. the EEG Inaccessibility makes it difficult to track the seizure in real time, analyze and pave the way to predict patients' seizures in the future.

In contrast to EEG, nowadays, ECG measurements are more common in point of care systems such as watches which are already popular in the market.

Our aim is to automatically detect the epileptic seizures' periods using heart rate variability features to accelerate the analysis by the expert, moreover we want to use machine learning methods to evaluate our ability to predict future seizures based on the data available to us.

**Methods:** At first, we performed peak-detection algorithm benchmarking to choose a peak detector to be used in our system from the ECG detectors python library. The benchmark was done using the MIT-BIH Arrhythmia Database, which contains reference beat annotations.

Extracting HRV (Heart Rate Variability) features in time and frequency domain.

**Results:** After preprocessing the ECG segments and detecting the R-peaks peak detector benchmark we used peak detector benchmark to be based on in the detector selection (Engzee), then calculate RR interval time series, which is computed from the time differences between consecutive R-peaks. The next step was extracting HRV features in time and frequency domain, the decision-making process taken for the seizures detection is performed using Machine-Learning methods.

**Conclusions:** Using HRV analysis seems to be a reliable method for non-invasive seizures detection. In the present study, an algorithm for detection and classification of epileptic seizures and non-epileptic segments is performed.

The methodology proposed in this paper can be used to improve monitoring systems for detection of epileptic seizures, enhance doctors' cost-effectiveness and reducing the impact of epilepsy on the patients' quality of life.

**Keywords:** Epilepsy, ECG, RR-Intervals, Epileptic Seizures.

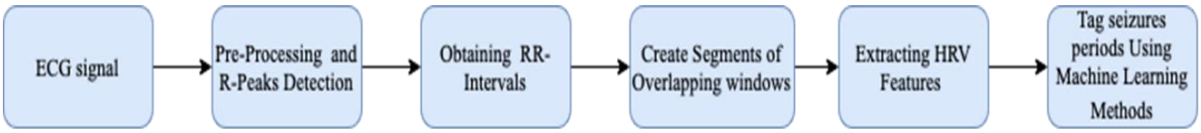


**Figure 1.** flow diagram of the proposed methodology. First, the ECG was inspected by identifying the R-peaks with 4 different detectors over 30 records and their performances were measured. Afterwards, the intervals between subsequent R-peaks were obtained yielding the RR intervals. The last step consisted of computing the HRV features and evaluate our ability to detect seizures' periods trough deep machine methods.

**(19)**

# A Physiological-Based Computerized Model of Cardiac Activity in Mice and Humans for Drug Development and Personalized Medicine

Nitay Aspis[1], Ofek Boneh[1], Ido Weiser Biton[1], Yael Yaniv[1]

[1] Faculty of Biomedical Engineering, Technion – IIT, Haifa, Israel

**Introduction:** The development of new drugs is a long and expensive process, and thus creates barriers to new discoveries and treatments. Such development includes pre-clinical and clinical studies, while the assessed drug may rise efficacy and safety issues during its examination. Therefore, there is a need for innovative research tools to evaluate new drugs at the beginning of their development in different physiological and genetic scenarios, and even to better select the patients that will benefit from them on personalized-medical basis. In this study, we focused on the effect of drugs on cardiac function and based on previous results that show a correlation between the heart rate variability (HRV) and physiological activity.

**Methods:** Here we offer a novel tool to evaluate the activity of drugs on pre-clinical (mouse) and clinical (human induced pluripotent stem cells, hiPSC) models by using in-silico computational models of cardiomyocytes. We used the Arbel-Ganon et al. model as a mouse model and the Grandi, E. et al. model which models hiPSC, and inserted into them, for the first time to the best of our knowledge, random noise to several parameters. Thus, we created a physiological cardiac model that has variation and better represents cardiac electrophysiology.

**Results:** For both models, the original HRV parameters were extremely different from the in-vivo cells' measures. As predicted, adding noise to the physiological parameters within each model increased the variability, and after fine-tuning any noise vector amplitude, both statistics (mean, STD), linear (histogram), and non-linear (MSE) measures behaved as the physiological measurements.

**Conclusions:** Our model can already now be implemented for different genetic variations and represent mouse and human physiology, thus, improving and shortening the developmental process of new drugs and enabling the physicians and pharmacy companies to better select patients for existing medications. Future development of these models would possibly open the door also for calculating drug-drug interactions, predicting adverse effects of drugs on heart activity, and simulating the interaction between medications and age-related physiological modulations to enable personalized medicine and drug adjustments.

**Keywords:** Heart rate, cardiac, heart activity model, noise, heart rate variation, HRV, in-silico model.

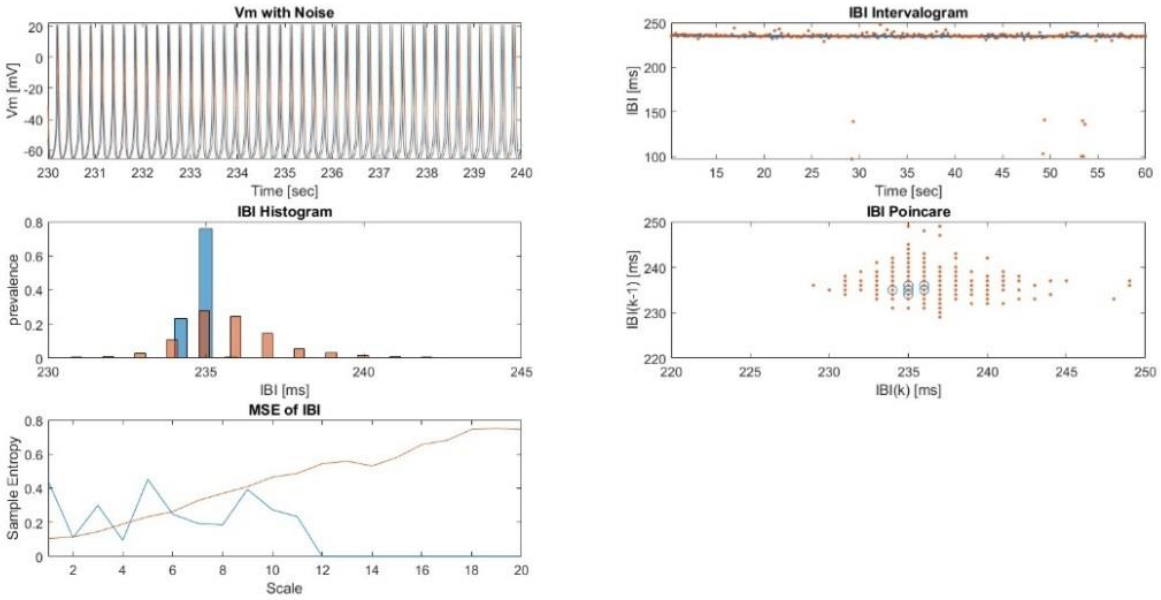


**Figure 1:** Mouse model – comparison between deterministic and stochastic outputs. The original output is presented in blue, noisy output is presented in red. The added variability by the noise is visible at the intervalogram and at the histogram plots. The change in the MSE measure is also visible.

**(20)**

# Wearable Device for Epileptic Seizure Detection and Prediction

Mais Hadid[1], Sabry Assaf[1], Noam Keidar[1], Galya Segal[1]

[1] Faculty of Biomedical Engineering, Technion - IIT, Haifa, Israel

**Introduction:** Epilepsy is a chronic noncommunicable disease of the brain that affects around 50 million people worldwide. It is characterized by recurrent seizures, and can have a broad spectrum of social consequences, impair quality of life and create psychosocial problems.

Considerable part of the disease burden is attributed to the unexpectable nature of seizures, thus automatic detection of events may facilitate early detection, timely intervention, and reduce the impact of epilepsy on patients' lives.

In order to build a device of real time signal acquisition and algorithm testing experiment system, we set some system requirement specifications, that are: frequency sample of 256Hz, 5 EEG channels, Real-time data acquisition, raw data accessibility, flexibility of electrode placement, approved for clinical trials, safe to use, comfortable and useable everywhere. We built a device that fulfills these requirements and satisfies the needs for clinical trails in Israel, as it satisfies all Helsinki committee requirements and is safe to use.

**Methods:** First, we chose which components will make up the device according to our project's requirements, as stated above: Electrodes – we wanted dry and flexible electrodes, so we chose dry comb electrodes. Along we chose the electrodes band because it was suitable for our electrodes. Board – we wanted a board that analyzes 5 channels of EEG and 3 ECG signals, so we chose Cyton Board by OpenBCI, in addition to the dongle that comes along.

Second, we developed a real-time signal acquisition and algorithm testing experiment system for seizure detection and prediction trails using python, that saves the results and the signals acquired. We also built a GUI as a web app that presents the result of the algorithm for the user.

**Results:** we were able to build a comfortable and easy to wear system that acquires real-time EEG data with 0.1s latency, that records 5 EEG channels simultaneously, the experiment can last for hours and even days, as the system relies on AAA batteries and not rechargeable ones, the signals are processed it in order to detect or predict an epileptic seizure.

**Conclusions:** We built an experiment system that fulfill the specifications for the clinical trial.

**Keywords:** epilepsy, detection, prediction, EEG, real time.

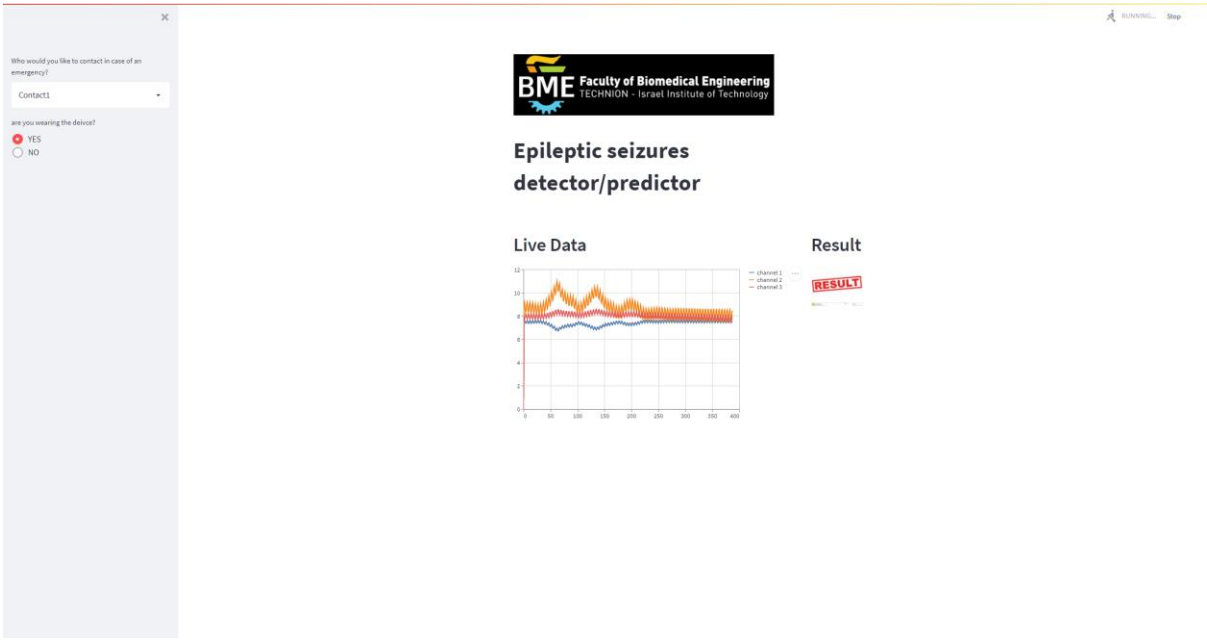


**Figure 1.** The graphical user interface (GUI) we built for our technology, real-time data is plotted on the right, and the result of the detection/prediction algorithm is on the left.

**(21)**

# Finding A Synergistic Combination of Drugs for The Treatment of Head and Neck Cancer

Yuval Ganot[1], Smadar Alon[1], Asaf Eilon[1], Dana Meron Azagury[1], Yosi Shamay[1]

[1] Faculty of Biomedical Engineering, Technion - IIT, Haifa, Israel

**Introduction:** Every year, approximately 900,000 cancer cases and over 400,000 deaths are caused by Head and Neck cancers. Today, there are several methods for treating head and neck cancers, including surgery, radiation therapy, chemotherapy, targeted therapy, immunotherapy, or a combination of these treatments. Treatments today have a wide range of severe side effects, which significantly impair the lifestyle of those suffering from the disease. This study uses innovative technology, which includes the use of nanoparticles to create a more effective treatment. Our goal is to find synergistic combinations of drugs for the treatment of head and neck cancer and use prediction and innovative technology of creating nanoparticles from several drugs to significantly reduce side effects. We will find leading combinations of drugs in 2D, and afterwards will test them in 3D.

**Methods:** First, we searched for relevant drugs to test. With spike4cancer program, we can input drugs for our choice and see relevant research regard combinations of those drugs. We managed to find 15 combinations which we tested with 2D High throughput screening. In order to determine the number of living cells left, we used statistical analysis. The next stage was to determine the synergy scores of the combinations using the ZIP calculation method. We then moved on to a 3D tumor spheroid model to determine the ability of the drugs to penetrate solid tumors. Afterwards, we formulated NPs using the nano-precipitation to encapsulate the final combinations, and tested the NPs quality and effectiveness using statistical analysis such as DLS and HPLC.

**Results:** From 15 combinations, we chose the top 3 which yielded the best results. We then calculated the synergy scores of these three combinations. Continuing to 3D with those 3 combinations did not give results as expected, most likely because the drugs could not effectively penetrate solid tumors. We moved on to try the combination of three drugs, due to the high toxicity of the drugs we encapsulated 2 of them in NPs. We tried different methods with different combinations of the drugs to optimize the NPs. The NPswere well made and had good size distribution and Polydispersity index. Our final results using NPs and free drug on 3D FaDu cells did not show efficacy of any combinations in NPs over the use of a single drug as free drug.

**Conclusions:** Biological research, such as testing synergists with drugs, requires a lot of testing to determine the best combination. We studied the aspect of personalized medicine and the adjustments of drugs to different types of cancer. As with any biological experiment, the results may not be ideal. In this case, our results in 3D were not as good as 2D so while we found a

combination that makes good NPs, it did not have a good effect on H&N cancer cells. For better results, further hightroughput drug combination screening is required in this field of research. Effectively choosing combinations without long testing would be a breakthrough.

**Keywords:** Synergism, Combination, Cancer, Nanoparticles.

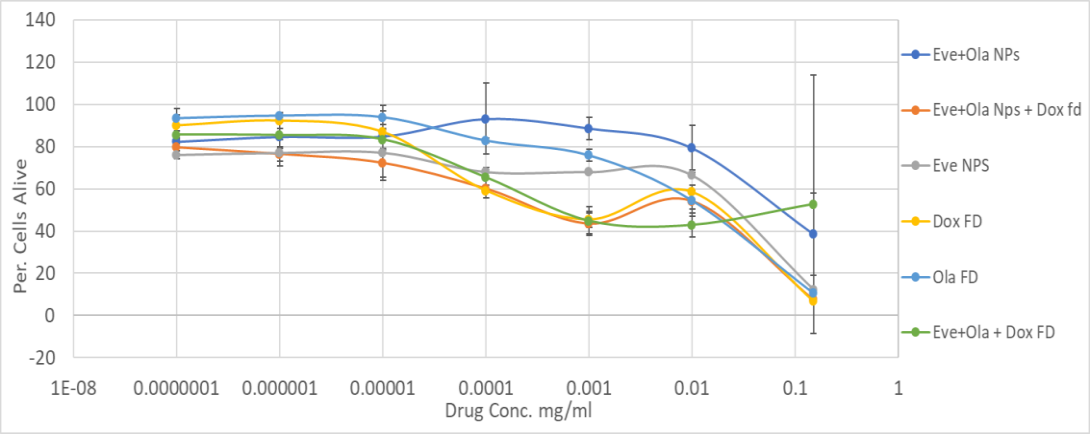


**Figure 1.** Testing different combinations in 3D using nanoparticles. In the figure, the different methods of creating nanoparticles are compared. As can be seen, our nanoparticles have not shown significant advantage over the single drugs as free drugs.

**(22)**

# Dyslexia Detection with fMRI Scans Using Machine Learning

Rotem Gatenyo[1], Emmanuelle Hadjadj[1], Nikolay Taran[2], Tzipi Horowitz-Kraus[2]

[1] Faculty of Biomedical Engineering, Technion - IIT, Haifa, Israel
[2] Faculty of Education in Science and Technology, Technion - IIT, Haifa, Israel

**Introduction:** Dyslexia is the most common learning disability (~8% prevalence), a neurodevelopmental disorder that mainly affects reading impairment. Dyslexia is usually diagnosed after 2-3 years, or later, of formal schooling. This late diagnosis puts the children with dyslexia at an academic disadvantage and may also lead to psychiatric disorders such as anxiety and depression. Functional Magnetic Resonance Imaging (fMRI) measures brain activation in neural blood oxygen-level under varying cognitive conditions and is a potential tool to detect dyslexia. Based on a series of multi-slice images of the brain, fMRI provides the functional information of detecting and analyzing different parts of the brain. Machine-learning (ML) has led to breakthrough innovations in diagnostics, due to its ability to use various algorithms to teach computers to find data patterns for future predictions and classifications, thus, an effective tool to classify subjects with dyslexia.

**Methods:** The data, resting-state fMRI images from 118 children; 52 typical readers (TR) and 66 children with dyslexia was preprocessed using SPM-12 toolbox. The preprocessing of the fMRI scans included realignment of the data to correct motion by unifying data orientation, coregistration of the anatomical MRI images to the functional MRI images and normalization of all coregistered images to the Montreal Neurological Institute template. Additionally, segmentation was performed by mapping the tissues of the anatomical images to different tissues (e.g., gray matter, white matter and cerebrospinal fluid). Furthermore, spatial smoothing using an 8-mm Gaussian kernel. Finally, global artifacts were removed using Global Signal Regression.

The ML model's features are the correlation coefficients between all regions of interest (ROI) (Figure 1), while we used one group of ROIs at a time for classification; cingulo-opercular and frontoparietal connectivity, dorsal and ventral attention network connectivity, default mode network connectivity, and a control group - Sensory motor hand. Feature selection was performed to reduce the number of features to be more manageable for processing. For classification, Support Vector Machine, Linear Regression and Random Forest classifiers were used to distinguish between TR and children with dyslexia.

**Results:** The best performance was achieved by extracting the features from the Ventral Attention Network with 83% accuracy and 85% F1 and from the Dorsal Attention network with 79% accuracy and 82% F1. The control group features were extracted from the Sensory Motor Mouth and showed the poorest results with 50% accuracy and 64% F1.

**Conclusions:** The purpose of this study is to detect children with dyslexia based on rs-fMRI scans using machine-learning tools. The Ventral Attention Network and Dorsal Attention Network models have appropriately categorized TR and dyslexia patients. These results may indicate that the biggest neurobiological differences between TR and children with dyslexia are located in attention-related brain networks. Due to the limited number of participants further data acquisition is needed as well as, a more thorough analysis of sub-regions of selected brain regions where the activation difference is even more

significant. When higher results are achieved, the model can allow diagnosis of other neurological disorders such as Autism.

**Keywords:** fMRI; Machine Learning; Functional Connectivity; Dyslexia.

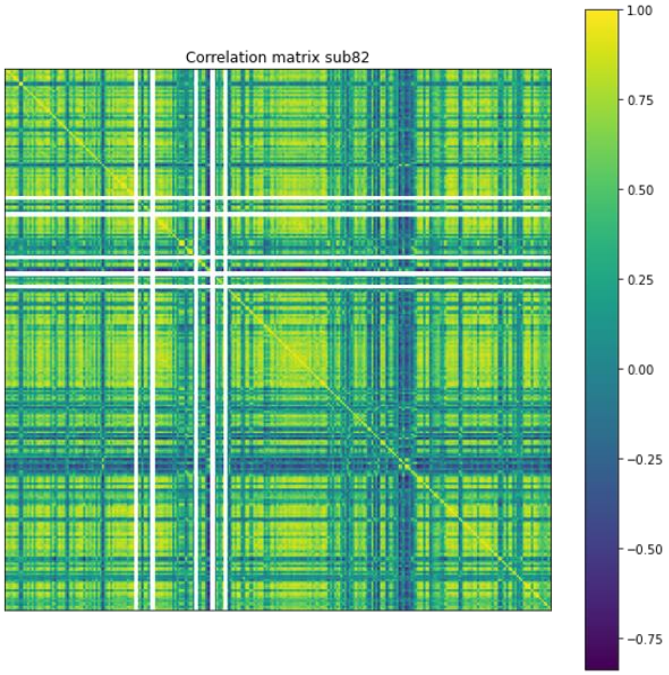


**Figure 1.** correlation matrix of a random patient, representing the correlation coefficients between all regions of interest.

**(23)**

# "Tumorosomes" - Tumor Biomimetic Nanoparticles for Triple-Negative Breast Cancer Targeting

Ofri Vizenblit[1], Noga Erez[1], Assaf Zinger[2,3]

[1] Faculty of Biomedical Engineering, Technion - IIT, Haifa, Israel
[2] Faculty of Chemical Engineering, Technion - IIT, Haifa, Israel
[3] Cardiovascular Sciences and Neurosurgery Departments, Houston Methodist Academic Institute, TX, USA

**Introduction:** Triple-negative breast cancer is the most aggressive subtype of breast cancer with a local recurrence rate of up to 72% in 5 years. In the metastatic setting, the 5-year overall survival is 12%. Due to the lack of common hormone receptors, there is difficulty in developing targeted therapies. Despite significant increases in knowledge, there has been limited progress made in the clinically approved treatments of Triple-negative breast cancer, leaving chemotherapy as the gold medical standard for systemic therapy in the neoadjuvant and metastatic settings. Thus, there is an urgent need to develop specific theranostic tools for early cancer diagnosis and efficient cancer-targeted treatment. Biomimetic strategies represent a paradigm shift in the design of nanoparticles, enabling next-generation platforms capable of effectively interacting with complex biological systems through biomimicry of native cells. Taking these insights in mind, nanoparticles coated with tumor-specific membrane proteins can mimic tumor cells' behavior in the tumor's complex microenvironment and may adhere to other cells during malignant development. Here we have designed and characterized biomimetic, tumor cells' membrane proteins-based nanoparticles, called "Tumorosomes", that could potentially serve as an effective theranostic tool for Triple-negative breast cancer.

**Methods:** First we cultured 4T1 cancer cells. Next, we performed membrane proteins extraction procedure using a commercial kit and further protein quantification using Rapid Gold BCA assay. Then, we fabricated Tumorosomes and Liposomes using ethanol injection procedure, including organic and aqueous phases preparation, followed by extrusion and overnight dialysis. For further *in-vitro* nanoparticles tracking, rhodamine-labeled lipids were added to the organic phase. After fabrication, we measured the size, polydispersity index, and zeta potential of the nanoparticles using Zetasizer Nano. Finally, we performed an *in-vitro* association assessment of nanoparticles with 4T1 cancer cells using IncuCyte imaging, including phase-contrast and red fluorescence channels. 4T1 cells assay was treated with 0.1, 0.2, 0.5-, and 1-mM nanoparticle concentrations compared to untreated control. Fluorescence intensity was analyzed using IncuCyte ZOOM software and statistical analysis was performed using GraphPad 9.3.1 software.

**Results:** Nanoparticles were fabricated using protein: lipid ratio (w/w) of 1:40. After fabrication, all nanoparticles underwent physicochemical characterization, size, polydispersity index, and zeta potential measurements results are shown in **Table 1**. Finally, the mean fluorescence intensity was evaluated using IncuCyte for the different nanoparticles'

concentrations. The mean fluorescence intensity of Tumorosomes was significantly higher ($P < 0.01$) than Liposomes in 1mM nanoparticles' concentration.

| **Measurement** | **Tumorosomes** | **Liposomes** |
|---|---|---|
| Size [nm] | 79.0 ± 2.8 | 79.8 ± 0.4 |
| Polydispersity Index [a.u] | 0.109 ± 0.02 | 0.109 ± 0.02 |
| Zeta Potential [mV] | -4.94 ± 0.80 | -3.89 ± 0.15 |

**Table 1.** DLS measurements results.

**Conclusions:** Tumorosomes induce a higher association with 4T1 cancer cells than conventional Liposomes. Furthermore, Tumorosomes present the same physiochemical characteristics as conventional, FDA-approved Liposomes, with a size smaller than 100 nm and a slightly negative charge. Thus, herein we developed an innovative nanoparticles design, that could initiate *in-vivo* preclinical future research for cancer treatment and early diagnosis.

**Keywords:** Breast Cancer, Nanomedicine, Biomimicry, Liposomes.

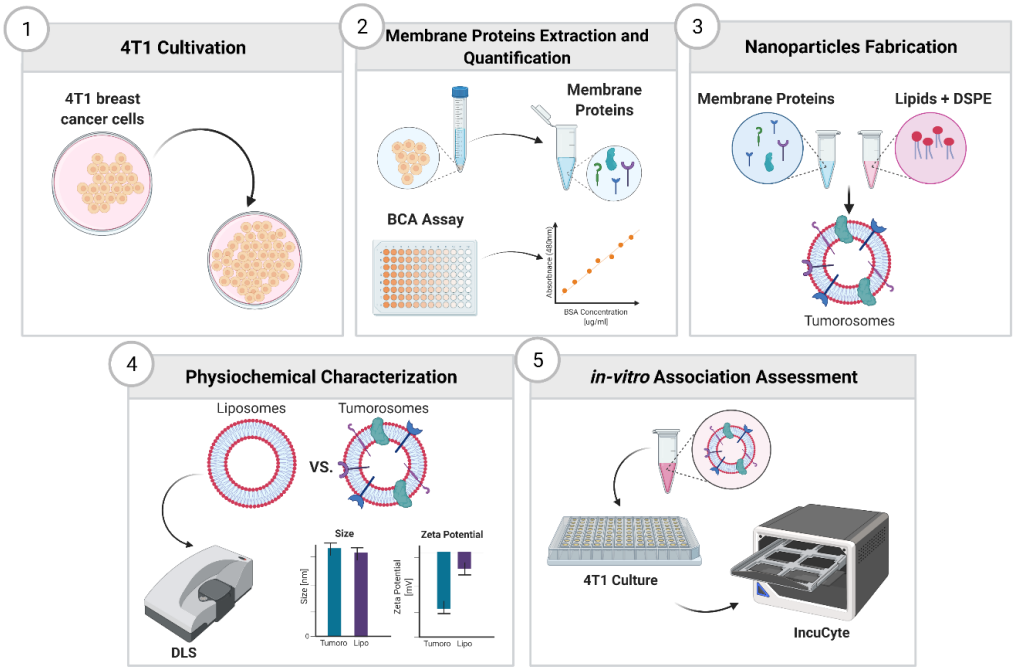


**Figure 1.** Project workflow illustration, Created with BioRender.com.

**(24)**

# Machine Learning Based Analysis of Spatial Behavior as A Biomarker for Aging

Hiba Abu-Rajab[1], Asael Melchior[1], Moti Freiman[1], Michal Isaacson[2]

[1] Faculty of Biomedical Engineering, Technion - IIT, Haifa, Israel
[2] Haifa University, Israel

**Introduction:** It is obvious that we are living in an era ruled by technology and mobile phones, calculating every move, and step that individual proceeds, looking at the technology that we have in recent years and the rapid development in addition to the availability of small, inexpensive, and reliable tracking devices has led to a growing volume of research that uses this technology as a tool for data collection in various disciplines. Many researchers focused on the correlativity between spatial activity and human mental\physical wellbeing. In this project, we examined GPS data (spatial activity) of patients using observational approaches, activity monitoring, or behavioral checklists to create a tool that will help predict cognitively physically patients' health as part of ongoing research at Haifa's university. we built an ML-based tool to assist in analyzing previously collected data as part of her research of cognitive \physical disorders; for instance, tracking the healing process of a patient after a spine surgery

**Methods:** We examined_ GPS signals for 400 different days and from 15 different people we analyzed with different statistical tools to find the most effective features for our ML model and 3 different models were examined to get the best result, after developing about 20 features we chose the 5 most affective features(<5% for the model decision): the first gradient of the trajectory, the second gradient of the trajectory, the angel of the trajectory, the signal scatter STD, and the signal scatter mean (for every 10 signals). We moved on to choose our model after examining logistic regression, k-mean (an unsupervised model), and random forest we found out that we get the best results with random forest and fin-tuned it to get the best results. Afterward, we worked on our UI so it can be accessible, we worked with Streamlit package in python and uploaded our results online for the lab at Haifa university to use.

**Results:** eventually, we received a model with results of F1=0.82 and AUC=0.948 and an Accuracy of 90% which are reliable results in the ML world furthermore our tool got very positive feedback from the researchers at Haifa University, therefore, they are applying it in their research.

**Conclusions:** We believe that with the tool we built researchers can further investigate the field of using the spatial activity of the patients to predict cognitively physical patients' health in a more affection and accurate way.

**Keywords:** Machine learning, GPS data, Spatial activity, Spine surgery, Cognitive disorders

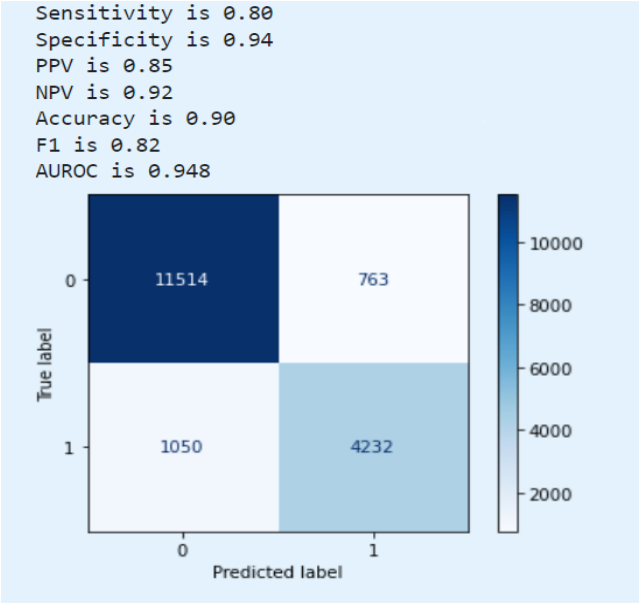


**Figure 1.** Heat map and results of Random Forest model.

**(25)**

# Non-Invasive Monitoring and Detection of Arterial Stenosis Severity and Location – A Clinical Feasibility Study

Dana Farah[1], Fadi Haddad[1], Tomer Heitner[1], Amir Landesberg[1]

[1] Faculty of Biomedical Engineering, Technion - IIT, Haifa, Israel

**Introduction:** Peripheral Artery Disease (PAD) affects over 200 million people worldwide with life-limiting symptoms, that may even require lower limb amputation. The Ankle Brachial Index (ABI), the ratio of the ankle to brachial peak systolic pressure, is the prominent non-invasive modality for assessment and monitoring of patients, but suffers from low sensitivity, especially in elderly and diabetics due to widespread arteriosclerosis. In recent clinical studies, we have shown the superiority of a novel modality that utilizes Impedance Plethysmography to measure changes in perfusion dynamics (PD) to monitor PAD patients. Prolongation of the upstroke of the perfusion wave measured below the knee (BK), as quantified in the maximum acceleration time (MAT) and Perfusion Delay Index (PDI), can detect above-knee (AK) stenosis with 91% sensitivity and 85% specificity. BK stenosis detection using PD was not attempted, we hypothesized that measuring PD distal to the site of stenosis will enable its detection, while proximal PD measurement will not, and measurement at several sites may assist in the localization of the lesion and in clinical decision making.

**Methods:** In a Helsinki-approved clinical trial we measured PD signals from the calves and feet of healthy students. Stenosis was emulated utilizing a pressure cuff on the thigh or calf. The cuff was inflated to 10 mmHg below the measured ankle diastolic pressure. After three minutes of baseline recording, three phases of emulated stenosis were performed at the calf, thigh or both. Each stenosis phase lasted three minutes and was followed by a three minutes recovery phase. The PD signals were processed to achieve a characteristic perfusion dynamics wave, which was analyzed using proprietary Matlab software. The PDI, Maximum Acceleration Time (MAT) and other PD indices were calculated and compared between the different phases.

**Results and Discussion:** Twenty-four healthy participants were recruited. Prolongation of the MAT was observed during thigh emulated stenosis in both calf and feet, as observed in earlier trials. The MAT prolonged from 231±17ms to 309±24ms ($P<0.01$) in the calf and from 261±20 ms to 337±23 ms ($P<0.01$) in the feet. Emulated stenosis in the calf, however, yielded different patterns in the calf and feet. The MAT in the foot prolonged from 261±20 ms to 321±36 ms ($P<0.01$) while there were no significant differences in the calf (231±17ms at baseline vs 235±19 ms, $P=0.0284$ at calf stenosis).

**Conclusions:** This study emphasizes the significance of correctly determining the site of PD measurement for the detection of stenosis. Stenosis in the thigh was detected when measuring PD signals from the calf or the foot, while Stenosis in the calf was detected only by measuring PD in the foot. Altogether, measuring PD distal to the site of stenosis will enable its detection, while measuring proximal to the site of stenosis will most likely give rise to an undesired false-

negative result. This novel concept should be further tested and validated in clinical trials in PAD patients.

**Keywords:** Peripheral artery disease, maximum acceleration time, ankle-brachial index.

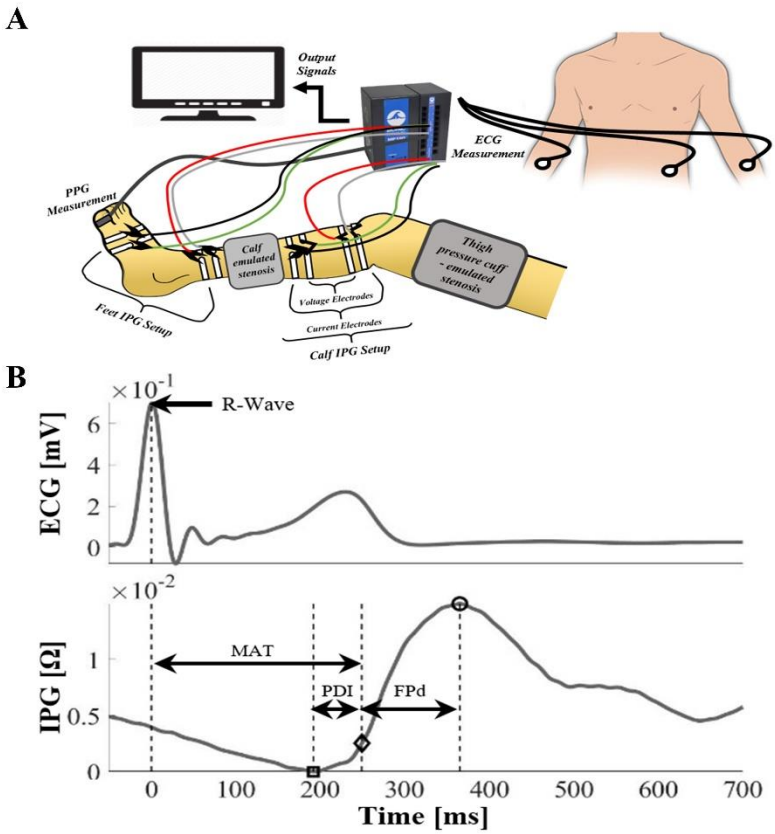


**Figure 1.** The experimental setup (A) included simultaneous measurements of Impedance Plethysmography (IPG) at the calf and feet, Photoplethysmography (PPG) from the toe and ECG. Stenoses were emulated utilizing pressure cuffs on the thigh and calf. Processing of the IPG perfusion signals yielded a characteristic perfusion dynamics wave (B-Bottom). The Maximum Acceleration Time (MAT - ◊), PDI and other novel indices were quantified and compared under various conditions.

**(26)**

# Investigating Microparticles for Biophysical Targeting of Abdominal Aortic Aneurysms

Perla Namour[1], Ido Rachbuch[1], Moran Levi[1], Yevgeniy Kreinin[1], Merav Belenkovich[1], Netanel Korin[1]

[1] Faculty of Biomedical Engineering, Technion - IIT, Haifa, Israel

**Introduction:** Abdominal Aortic Aneurysm (AAA) is a localized dilatation of the infrarenal aorta. It is a multifactorial disease that in advanced stages may result in rupture, leading to a life-threatening internal hemorrhage with high mortality rates. Since intact AAAs are mostly asymptomatic, diagnosing the disease and assessing rupture risk is challenging. Patients with a high risk are offered a preventive repair procedure with either open surgery or endovascular aortic repair (EVAR), which is less invasive but not compatible for all. These procedures are not optimal and are often related to significant complications.

Here, we offer an alternative paradigm by demonstrating the feasibility of an efficient transport system for targeted delivery of diagnostic or therapeutic agents to AAA sites. We aim to utilize the unique flow patterns (low shear rate, vortices) and biological features (exposed collagen and inflamed endothelial cells) that characterize AAAs as a biophysical targeting mechanism.

**Methods:** We designed and fabricated silicone *in-vitro* models of murine and human AAAs based on real imaging data, using 3D printing and sacrificial materials. The inner cavity of the models was coated with either human collagen or a layer of human endothelial cells (ECs). To mimic physiological flow conditions, we used a closed-circuit perfusion system based on a peristaltic pump, a fluid reservoir, a damper and appropriate tubing. Additionally, for better understanding of the theoretical flow patterns, we generated computational fluid dynamics (CFD) models and extracted important data including streamlines and wall shear maps.

Fluorescent carboxylate-modified polystyrene microspheres were covalently bound to Dimeric Glycoprotein VI-FC (GPVI) – a biological targeting moiety which binds to collagen. The particles were perfused into both types of models (collagen coated or EC coated) in PBS solutions at physiological flow rate for 1 hour. Particle accumulation at the vessel walls was observed and recorded with a fluorescent microscope during and after perfusion. Final images of idle adhered particles were processed (Python) to display and measure particle distribution.

**Results:** $2\mu m$ microparticles coupled with GPVI accumulate preferably on exposed collagen at the dilated wall of AAA sites, while avoiding EC coated areas and normal diameter (healthy) regions. Our CFD simulations correlate to these findings by showing circular flow patterns and low wall shear at the targeted site.

**Conclusions:** We developed a system that simulates the physiological conditions of AAA sites *in-vitro*, allowing to examine different types of targeted particles under accurately selected conditions. Our results show that the unique flow characteristics at AAAs direct microparticles

into the vessel wall at low velocities and shear rates, enabling specific local accumulation. Particularly, GPVI-coupling promotes particle adherence at exposed collagen regions. Additional targeting moieties and other parameters like particle size can be evaluated with this set up, leading to an optimized delivery system for diagnostic and therapeutic agents.

**Keywords:** Abdominal Aortic Aneurysm (AAA), Targeted Drug Delivery, Fluid Dynamics, Fluorescence Microscopy.

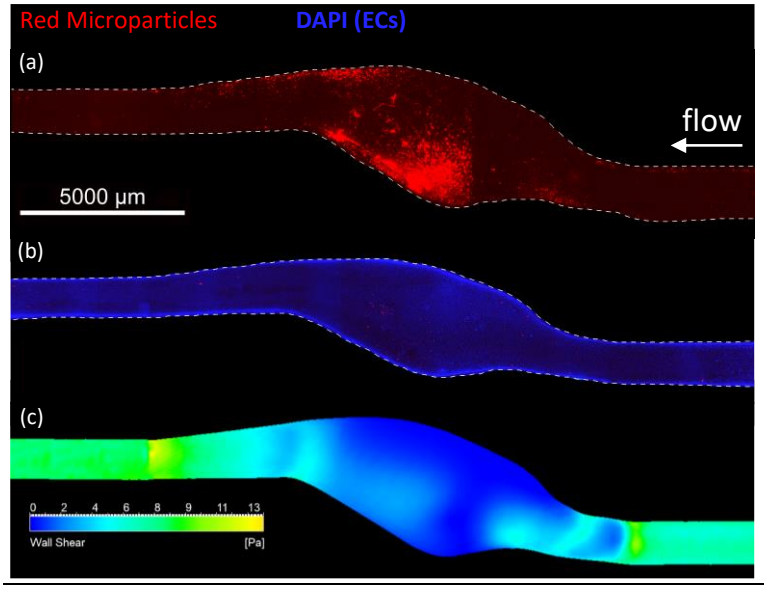


**Figure 1.** GPVI coupled fluorescent microparticles (red) deposition at the wall of a collagen coated (a) and EC coated (b) mouse AAA model. (c) Wall shear map at the corresponding AAA wall (CFD simulation).

**(27)**

# Gait Tracking with Wearable IMU Sensors

Keren Ashour[1], Avital Spector[1], Hilik Harari[2], Merav Belenkovich[1], Zvika Shinar[3]

[1] Faculty of Biomedical Engineering, Technion - IIT, Haifa, Israel
[2] GaitBetter – wellness and fitness services
[3] MindUP – digital health incubator

**Introduction:** Falling is a common phenomenon and a big problem amongst the elderly. For this population, recovery is slower and more difficult than average population, and therefore requires advanced solutions to prevent such injuries. These issues raise the need to train elderly patients with walking difficulties to improve their balance and performance when walking. The combination of cognitive and strength training, together with visual feedback, was proven to increase effectiveness of the training. GaitBetter uses a depth camera to recognize different gait phases and integrate them visually into a walking practice. This way the patients receive visual feedback for their performance in real time. Due to limitations in the current method, it was decided to explore the possibility for gait tracking with IMU sensors instead of depth camera.

**Methods:** Calibration was performed on the purchased sensors for the acceleration and magnetometer components. The calibration method relies on the gravitational and magnetic fields in the place where the measurements were performed. Pitch and roll orientation tracking over time was calculated from raw acceleration data using trigonometry methods. Similarly, yaw orientation over time was calculated from raw magnetometer data and trigonometry. Horizontal and vertical position over time were calculated using double integration of acceleration data, along with chosen filtration and processing methods. Robustness of the algorithm to different velocities was also examined.

**Results:** Pitch and roll results had deviations of up to 5 degrees, and yaw measurements had deviations of up to 10 degrees. Position results had less than 10% errors from measured values. It was found that for velocities less than $0.6\ \frac{km}{hour}$ accuracy of position was significantly reduced.

**Conclusions:** Highly accurate results of Euler angles and position can be achieved by using data from a wearable IMU sensor. There is a velocity limitation of the measurement to get accurate results, however this limitation is below walking velocity. Moreover, to get optimal results, the movement must be recorded and then analyzed offline with the algorithm developed.

**Keywords:** IMU sensors, Euler angles, position tracking, signal processing.

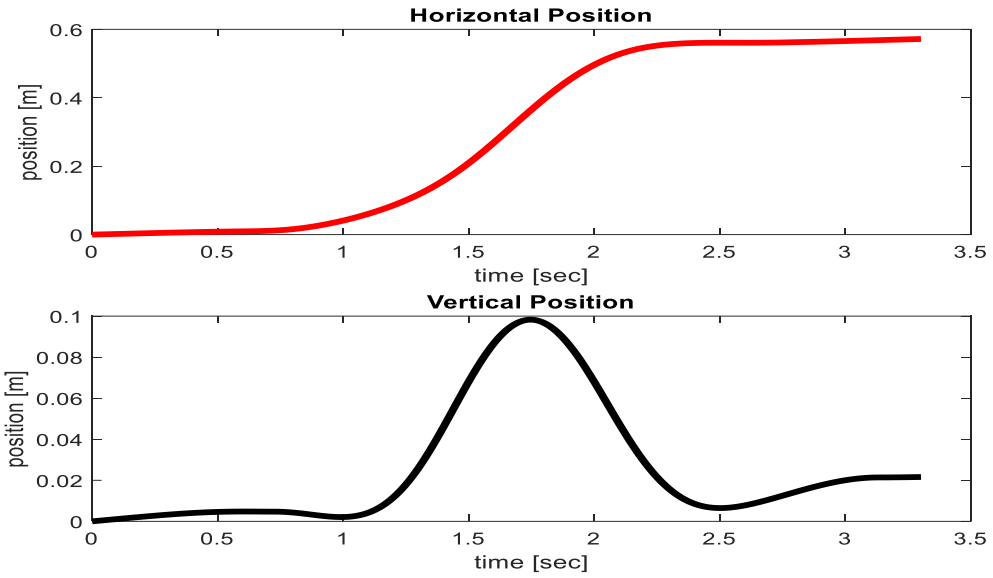


**Figure 1.** Horizontal and vertical positions of the sensor over time as acquired from the developed algorithm. Measured horizontal position was 60 cm and vertical position 10 cm.

**(28)**

# Finite Element Modeling of the Mechanical Interactions Associated with Cancer Cell Invasiveness

Lana Abdelghafer[1], Razan Zoabi[1], Marina Tulchinsky[1], Daphne Weihs[1]

[1] Faculty of Biomedical Engineering, Technion - IIT, Haifa, Israel

**Introduction:** The uncontrolled tumor progression-metastatic disease is the major clinical complication in most types of cancers and is considered the cause of more than 90% of cancer-related deaths. During cell invasion through the tissue- the critical step in the formation of metastasis, cells apply a normal force in addition to the traction force. Among the parameters affecting this force, hence the metastasis, is the cytoskeleton. Our main objective is to evaluate the effects of this parameter on the cell's capacity to indent the gel to estimate their ability to metastasize and invade distant sites in the body. Since indentation depth cannot be physically measured in the lab, we use FEBio software to simulate real experiments and measure it

**Methods:** Finite element models - To better understand the effect of the cell's mechanobiological aspects on their ability to metastasize, we model the real experiments in a new-designed finite element model. The model contains cells on a surface of an impenetrable, soft, elastic gel and an ellipsoid nucleus located in the ellipsoid void in the middle of the cell. To study the role of the cytoskeleton, we have defined a "tied facet-on-facet" contact in a ~38.38% area of the bottom part of the nucleus, representing actin filaments underneath the nucleus, and a "sliding facet-on-facet" contact to be in ~61.6% area of the rest of the nucleus to allow freedom movement of the nucleus, with a "tied facet-on-facet" contact between the cell and the gel to prevents surfaces from sliding or disconnecting (Sliding model). Total forces were defined in the range 100-300 nN to match the experimental range of traction forces applied by cancer cells on soft gels.

**Results:** The cytoskeleton-simulating model showed a positive correlation between the applied total force and the indentation depth of cells inside the gel, higher forces values resulted in deeper indentation measurements.

**Conclusions:** We propose that mechanobiological processes related to cytoskeleton organization including the force that the cytoskeleton applies on the cell, and distances between cells could have a major role in designing the invasive features of cancer cells and their ability to metastasize and invade distant sites in the body. This suggests that they may be valuable diagnostic or therapeutic tools to treat invasive cancers.

**Keywords:** Finite element modeling, Metastasis, Indentation Depths, Cytoskeleton.

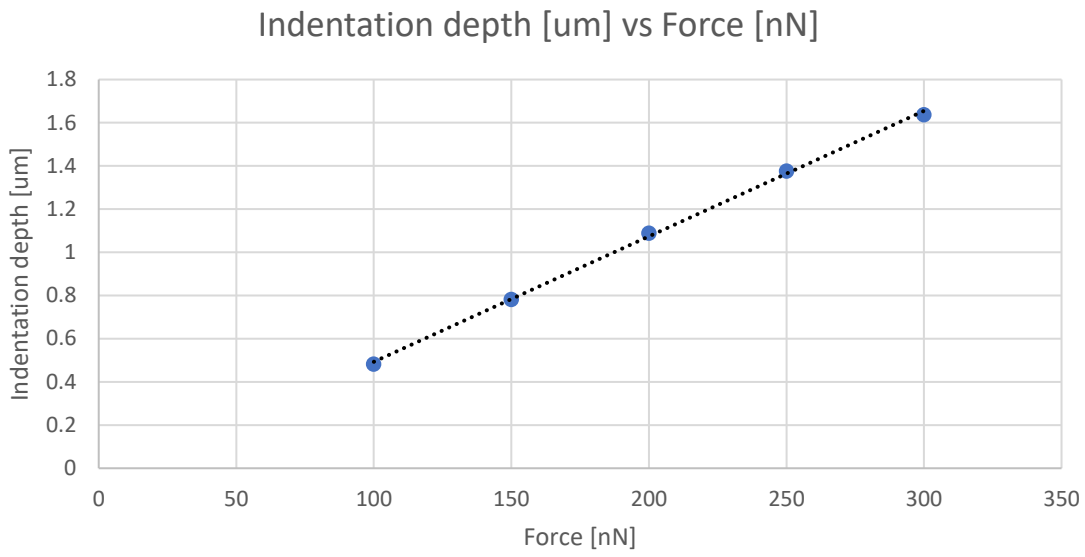


**Figure 1.** X-axis showing total force from 100nN to 300nN in steps of 50nN, Y-axis showing indentation depth [µm], Cell-induced indentation depths increase linearly with the total force magnitudes.

**(29)**

# Detection of Peripheral Arterial Stenosis by Non-Invasive Quantification of Perfusion Dynamics Utilizing Exercise Test

Hai Tkach[1], Shir Plotkin[1], Tomer Heitner[1], Amir Landsberg[1]

[1]Faculty of Biomedical Engineering, Technion - IIT, Haifa, Israel

**Introduction:** Peripheral artery disease (PAD) affects around 13% of the Western population over 50 years old. The Ankle Brachial Index (ABI) is the most common non-invasive diagnostic index to detect PAD. However, it suffers from low accuracy and sensitivity. Asymptomatic patients with mild or moderate stenosis may present with normal ABI due to low impedance to flow and small pressure gradient across the stenosis. In these patients post-exercise ABI is measured. Exercise induces distal arteriolar vasodilation, which reduces the post-stenosis blood pressure and the ABI. In recent clinical trials we introduced a novel modality for monitoring PAD by quantifying changes in perfusion dynamics (PD) measured using Impedance Plethysmography. Prolongation of the perfusion wave upstroke, as quantified in the Perfusion Delay Index (PDI) and Maximum Acceleration Time (MAT) was able to detect stenosis in patients with higher sensitivity than the ABI. We hypothesize that exercise in the presence of stenosis will yield pathognomonic changes in the perfusion wave that will enable even mild stenosis detection, which presents with normal ABI.

**Methods:** In a Helsinki-approved trial we measured PD signals from the calves of healthy students. A compression cuff induced emulated stenosis on the thigh. Every student underwent two measurements with a combination of compression pressures (40 or 60 mmHg) and exercise regime (Isometric or Cyclic). They performed plantar-flexion against a resistance band for a total duration of five minutes, and were allowed to rest with emulated stenosis for three minutes before and after the exercise phase. ABI was measured before and after induction of the emulated stenosis, and right after the exercise. Figure 1a illustrates the experimental setup.

**Results:** Fourteen healthy students were recruited and completed the study protocol. Initial results affirmed our previous observations, that emulated stenosis induces prolongation of the MAT and PDI, proportional to the severity of the stenosis. The MAT increased from 246±19 to 271±26 ms and from 242±17 to 297±27 ms at 40 mmHg and 60 mmHg compression respectively ($p<0.01$ for both). The most prominent change observed in the perfusion wave morphology after exercise with emulated stenosis, was widening of the wave. To quantify the widening, the Crest Width (CW) index was used at 80% of the maximal amplitude (Figure 1B), denoted CW80%. Normalizing the index by each subject heart rate (denoted perCW80%) produced a greater difference. The perCW80% increased from 15.2±2.8 to 18.4±5.4% ($p<0.01$) after exercise. Interestingly, the perCW80% was affected the most by cyclic exercise and increased from 14.8±2.0 to 18.1±2.8% ($p<0.01$). In the contralateral leg, cyclic exercise also induced significant CW widening. However, the change was not as substantial, from 14.4±2.0 to 16.4±2.6% ($p<0.01$). The ABI did not change significantly with emulated stenosis or after exercise.

**Conclusions:** As observed in previous trials, the MAT, a novel index of PD, can aid in detection and severity assessment of peripheral arterial stenosis. The perCW80%, also a novel index of PD which can aid in detection of legs with stenosis when measured after exercise. Future clinical studies in PAD patients are needed to validate the utility of the perCW80% index.

**Keywords:** Peripheral Artery Disease (PAD), Exercise, Impedance plethysmography (IPG), Ankle Branchial Index ABI.

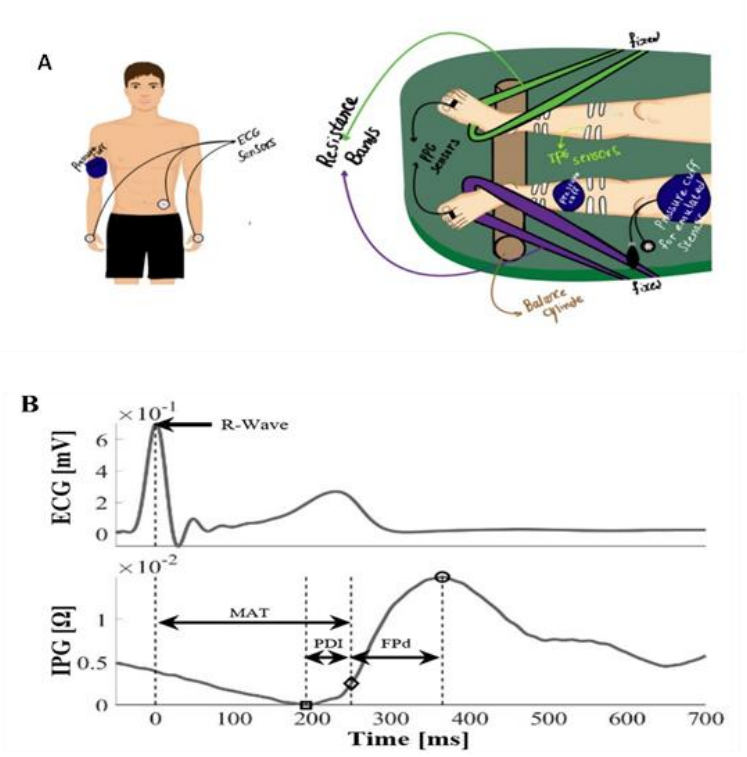


**Figure 1.** The experimental setup (A) included simultaneous measurements of Impedance Plethysmography (IPG) from both calves, Photoplethysmography (PPG) from both toes and ECG. Stenoses were emulated utilizing a pressure cuff on the thigh. Plantar-Flexion exercise was performed against a resistance silicone band. Blood pressure was measured in the arm and both ankles to calculate the ABI. Processing of the IPG perfusion signals yielded a characteristic perfusion dynamics wave (B-Bottom). The Maximum Acceleration Time (MAT - ◊), PDI, perCW80% and other novel indices were quantified and compared under various conditions.

**(30)**

# Middle-Ear Fluids Classification via Spectrally Encoded Endoscopy for Otitis Media Screening

Shira Weinrauch[1], Bar Davids[1], Matan Hamra[1], Merav Belenkovich[1]

[1] Faculty of Biomedical Engineering, Technion - IIT, Haifa, Israel

**Introduction:** Tympanic Membrane (TM) infections, are extremely common amongst children. Otitis Media (OM) is the most common, with over 80% of children developing it at least once [ref]. Due to high prevalence, OM is the leading reason for pediatrician visits, antibiotics prescriptions and surgeries at childhood. OM causes aggregation of fluid in the middle ear (ME) internal cavity, which causes mechanical deterioration of the TM, resulting in pain and, possibly, conductive hearing loss, unless treated on time. Hence, language development may delay amongst children. By using an optical setup to assess ME fluids' levels and viscosities, screening for OM and its severity may be performed non-invasively.

**Methods:** To model the TM during OM, a membrane was used as a TM analogue, and Glycerol-$H_2O$ solutions with varied viscosities were placed behind it at different levels (as an indicator of OM's development). Using Spectrally Encoded Endoscopy, films of the analogue's vibration under different external auditory stimulations were acquired. The frames were captured using a super luminescence polarization maintaining diode with 845 nm central wavelength and 50 nm bandwidth. The probe has a spatial resolution of 32x10 microns .We then acquired a scanline of each frame by averaging several pixels lines (perpendicular to the fluid surface) in the frame's center.

To determine the fluid level, we calculated the standard deviation (STD) of the scanline throughout the frames. By locating the first extremum start point of the STD line, we estimated the air-fluid boundary behind the membrane. We also created an evaluation test to identify uncertain estimations. To distinguish between different viscosities, we located the global maxima over time of each scanline, and followed its parameters differences: peak width, Fourier transform and STD.

**Results:** The fluid level estimation's success rate was 75% (**Error! Reference source not found.**), and the evaluation test's success rate was 64%. Viscosities classification based on the parameters mentioned didn't produce a proper correlation to the viscosities, though qualitative differences seem to be present such as scanline amplitudes.

| Known Fluid Level | Success Rate |
|---|---|
| 25 | 75% |
| 50 | 95% |
| 75 | 35% |
| 100 | 90% |

**Table 3**. Fluid level estimation performance per fluid level.

**Conclusions:** Challenges distinguishing between 50% and 75% fluid level caused a low success rate for estimating 75% fluid level. The best rate of level classification was achieved using 1000[Hz] stimulation, with 87.5% success rate and improved detection for 75% level.

Qualitative evaluation shows different behaviors between the low viscosities, but due to low SNR of high viscosities there's no definite conclusion. The viscosities used in the experiment are like OM pathology in adults but were an order of magnitude lower than those which may characterize severe OM in children. Optimizing a TM-analogue with lower surface tension may show better performance in highly viscous fluids while fitting for OM screening as per clinical accuracy and stimulation limitations.

**Keywords:** Tympanic-Membrane, Otitis-Media, Screening, SE-Endoscopy

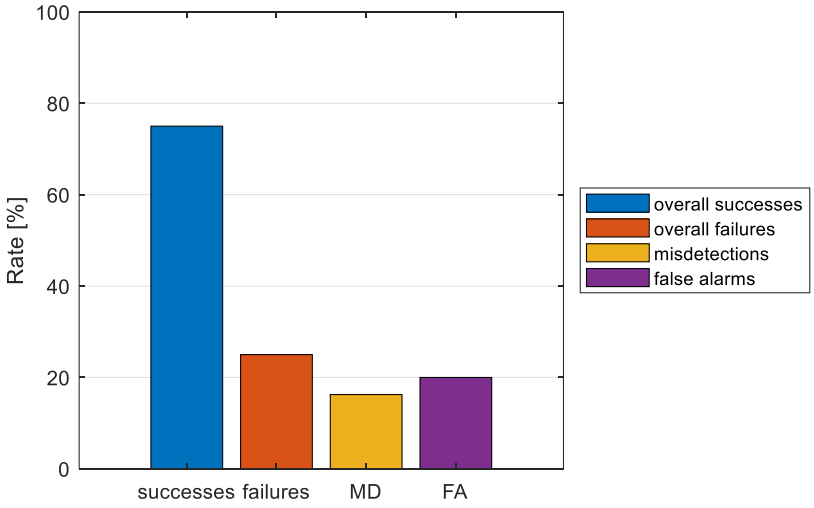


**Figure 1.** Fluid level estimation performance.

BME Biomedical Engineering TECHNION

TECHNION Israel Institute of Technology